Trajectory of a Spacecraft When It Passes by a Gravitational Body During Interstellar Travel

Larry M. Silverberg* and Jeffrey W. Eischen†
North Carolina State University, Raleigh, North Carolina 27695-7910

Interstellar space missions will require spacecraft that travel at relativistic speeds. Furthermore, their trajectories will be influenced by gravitational sources. Accordingly, this paper applies to interstellar missions a recently developed formulation of relativistic mechanics that predicts a spacecraft's trajectory when it passes by a gravitational source at a relativistic speed. The formulation, called spacetime impetus, is unique in that it employs a relativistic universal law of gravitation that does not explicitly require general relativity while producing precisely the same results. Based on these developments, an analyst can now update nonrelativistic mission planning codes to give them general relativistic capabilities. It requires augmenting the code with relativistic velocities and relativistic accelerations, the replacement of the universal law of gravitation with a relativistic universal law of gravitation, and setting up Lorentz transformations between frames.

Nomenclature

A, T, r_p, v_p, e	=	semimajor axis, orbital period, perihelion radius, perihelion velocity, and eccentricity
a, a_r, a_ϕ	=	magnitude, radial component and azimuthal component of acceleration
$a_R, a_{Rr}, a_{R\phi}$	=	magnitude, radial component, and azimuthal component of relativistic acceleration
α, b, v_b	=	for the general problem: entry angle, entry point, and entry speed
$a(r), b(r), u$	=	relativistic corrections in potential energy and force, and reciprocal of radial distance r
$D, \Delta\theta$	=	for the general problem: distance of travel and error in a calculated turn angle
dl, dx_r	=	length increment and spatial coordinate increments (where r is equal to 1, 2, 3)
$dt, d\tau, \gamma$	=	time increment, proper time increment, and Lorentz factor
$\boldsymbol{F}, \boldsymbol{P}$	=	interaction force vector and action force vector
$g_{rs}, g^{rs}, \Gamma^t_{rs}$	=	general relativity covariant metric coefficients, general relativity metric contravariant coefficients, and Christoffel symbols
H, h, μ	=	relativistic angular momentum, specific relativistic angular momentum, and reduced mass
M, m, G, g	=	for the general problem: source mass, spacecraft mass, universal gravitational constant, and acceleration due to gravity at the Earth's surface
M, M_A, R_S, R_A	=	for specific orbital mechanics problems: mass of the sun, mass of Alpha Centauri A, radius of the sun, and radius of Alpha Centauri A
R, B, θ	=	for the general problem: initial distance, impact parameter, and initial turn angle
$\boldsymbol{r}, \boldsymbol{v}, \boldsymbol{a}$	=	position vector, velocity vector, and acceleration vector
r, θ, ϕ, t	=	radial, polar, azimuthal, and time coordinates
$r_G, \theta_G, \phi_G, t_G$	=	radial, polar, azimuthal, and time coordinates for general relativity
r_s, c	=	Schwarzschild radius and speed of light
T, V, E, L	=	kinetic energy, potential energy, total energy, and Lagrangian
v, v_r, v_ϕ	=	magnitude, radial component and azimuthal component of velocity
$\boldsymbol{v}_R, \boldsymbol{a}_R$	=	relativistic velocity and acceleration vectors
$v_R, v_{Rr}, v_{R\phi}$	=	magnitude, radial component and azimuthal component of relativistic velocity
θ_f, t_f	=	for the general problem: flyby turn angle at a final time and flyby final time
ψ, ψ_R	=	acceleration angle and relativistic acceleration angle

I. Introduction

INTERSTELLAR missions that reach their destinations within a generation will require spacecraft that navigate across the cosmos at relativistic speeds. The planning for these missions will require simulation software that performs mission design tradeoff studies, energy and cost budgeting, astronavigation optimization, etc. In terms of the underlying physics, these codes will have to predict a spacecraft's relativistic trajectory as it passes by a gravitational source. This paper applies a new relativistic formulation of mechanics that can greatly simplify these predictions.

Interstellar missions are challenging primarily because of the distance of travel. Alpha Centauri, which is the star system that is closest to us and potentially habitable, is 4.3 light-years from our solar system (which is 268,000 AU, an AU being an astronomical unit equal to the distance between the sun and Earth). This is about 10,000 times larger than the size of our solar system (29.8 AU). The optimal interstellar mission begins with an acceleration phase that reaches a relativistic speed followed by a cruise phase. To get a sense of this, after a constant acceleration of 25 g's for about 2 days, a probe reaches a cruising speed of $0.15c$ when leaving the solar system. With that cruise speed, the probe reaches Alpha Centauri in about 30 years.

A number of propulsion systems are promising (e.g., electric propulsion [1], fission electric [2], and magnetic sails [3]), albeit electric propulsion, by itself, cannot increase the speed of a probe beyond $0.15c$. The feasibility of solar sail stability has been verified with a modest level of tensioning [4], methods of damage control from interstellar gas and dust have been suggested [5], and a system of multilayered materials has been proposed [6]. The nuclear laser pulse, in particular, does not require onboard fuel [7]. NASA has sponsored a number of feasibility studies, notably one by the Breakthrough Starshot Initiative [8], which is a laser-accelerated sailcraft. That study developed a relativistic model for straight motion under

*Professor, Mechanical and Aerospace Engineering; lmsilver@ncsu.edu (Corresponding Author).

†Professor Emeritus, Mechanical and Aerospace Engineering; eischen@ncsu.edu.

huge accelerations (order of 2500 g's) cruising at $0.2c$ after a 40 min acceleration phase over a distance of about 0.5 AU. That work examined a $0.01c$ precursor mission followed by the $0.2c$ mission. The accurate prediction of the interstellar trajectory's target depends on launch variabilities and gravitational effects during the journey [9]. Parkin [8] also raised the possibility that the risk from the bombardment of interstellar dust might necessitate sending a constellation of probes. A similar relativistic model was conducted for a sail that is only partially reflective [10]. That study also assumed that the motion is straight. They raised the future need to address "... telecommunication and astronavigation issues which must take into account several effects from general relativity," which result from the bending of the trajectory of a spacecraft and of light when passing by a gravitational source.

Understanding the impact properties of interstellar dust comes from in situ space experiments and models that balance the dust emission and extinction mechanism. The dust size and distribution [11,12] are most readily observable from the data. Predicting mass properties, which is critical to understanding the imposed stresses on a spacecraft, requires the difficult task of identifying dust species (e.g., [13,14]). As our understanding of the mass distribution continues to be studied, the need to plan for missions that avoid some dust bands seems certain. The Parker Solar Probe [15], which is currently orbiting close to the sun in a highly eccentric orbit, provides the most recent opportunity to examine the emission–extinction dust mechanism, and it also offers an opportunity to measure general relativistic effects on a spacecraft [16]. We estimated that the gravitational precession of the Parker Solar Probe orbit is 10 times greater than Mercury's gravitational precession, while Mercury's gravitational precession is greater than any other planet in our solar system (Appendix B).

The prediction of the trajectory of a spacecraft when it passes by a gravitational source is primarily a two-body problem of gravitational attraction between one massive, nonrotating, isotropic, uncharged body (the source) and a comparatively low-mass spacecraft. Trajectory changes range from a small perturbation in direction and speed of travel, a flyby, and an orbital insertion to a crash into the gravitational source. Analysts find these problems difficult to model because they require general relativity (GR), but also because GR is typically beyond the analyst's capabilities. The new relativistic mechanics formulation presented in this paper can treat these problems in a manner that avoids many of the present difficulties.

The new formulation is relativistic, and so it requires some relativistic notions but not those associated with GR. The new formulation is based on the theory of spacetime impetus (SI) [17]. Spacetime impetus uniquely bridges the gap between the Newtonian theory (NT), the theory of special relativity (SR), and GR. The SI connection to NT, SR, and GR is as follows: pertaining to NT, SI introduced a relativistic universal law of gravitation that originates with the universal law of gravitation in NT; pertaining to SR, SI employs the spacetime metric in SR; and pertaining to GR, the SI predictions are in full agreement with the Schwarzschild solution from GR. To implement SI, the mission analyst will need to convert a nonrelativistic formulation into a relativistic formulation. One codes the changes in a patched conic method or in any other such trajectory simulation and optimization code segments, where it would need to be augmented with relativistic velocities and relativistic accelerations, replace the universal law of gravitation with the relativistic universal law of gravitation, and set up Lorentz transformations between reference frames.

The following material is original and being presented here for the first time:

1) Nonexpert treatment: The paper was written for nonexperts in general relativistic mechanics.

2) The relativity triangle: We developed here a geometric interpretation of the relationship between relativistic acceleration and nonrelativistic acceleration, which turns out to take on the geometric form of a triangle (Sec. III). The added insight can assist the analyst.

3) Relativistic orbital mechanics: We present here four illustrative problems (three for spacecraft and one for light) (Sec. V).

4) Analytical verification: We provide here a discussion that motivated the advent of the relativistic universal law of gravitation.

We then explain why the new SI formulation and GR generate the same trajectories. A rigorous derivation introduces the mathematical mapping between SI and GR, from which one proves that the SI governing equations and GR governing equations are in full agreement (Appendix A).

5) Numerical verification: We examine the orbit of the Parker Solar Probe around the sun, in particular its precession. We solve the problem by SI and GR. This problem serves as a nice tutorial problem for those who seek to program the SI methodology. The code has also been made available [30].

The next three sections are preliminary; they review the concepts of relativistic velocity and relativistic acceleration, develop the relativity triangle and the relativistic gravitational law, and ultimately describe the governing equations of motion. The section after that solves the four illustrative relativistic orbital mechanics problems. The body of the paper ends with a summary of the results.

II.   Relativistic Velocity and Relativistic Acceleration

We begin by reviewing the concepts of relativistic velocity and relativistic acceleration (see Appendix A for more details of the following mathematical developments) [18]. In the nonrelativistic framework, the spatial distance increment dl between two points is constant across frames and is expressed mathematically by $dl^2 = dr \cdot dr$, where dr is an increment of the corresponding position vector between the points. The equation $dl^2 = dr \cdot dr$ is referred to as the spatial metric (invariant). Relativistic changes and nonrelativistic changes differ because relativistic changes account for the principle of light, and nonrelativistic changes do not. In accordance with the principle of light, one calibrates time measurement in a frame of reference relative to the speed of light. The speed of light is the same in each frame, which leads to relativistic differences across frames between spatial coordinates and temporal coordinates. Across frames, one holds constant a so-called proper time increment $d\tau$, expressed mathematically by

$$c^2 d\tau^2 = c^2 dt^2 - dl^2 \tag{1}$$

Equation (1) is referred to as the spacetime or Minkowski metric (invariant). It replaces the spatial metric employed in nonrelativistic problems. Dividing Eq. (1) by dt^2 yields $c^2 \geq v^2$, where $v = (dl/dt)$, which states that the speed of a body does not exceed the limiting value of c. One can also deduce from Eq. (1) that the speed c of light is the same across frames in accordance with the originally stated principle.

When invoking the principle of light, one defines the relativistic velocity vector $\boldsymbol{v}_R$ and the relativistic acceleration vector $\boldsymbol{a}_R$ as

$$\boldsymbol{v}_R = \frac{d\boldsymbol{r}}{d\tau} \tag{2a}$$

$$\boldsymbol{a}_R = \frac{d\boldsymbol{v}_R}{d\tau} \tag{2b}$$

Notice in Eq. (2) that the difference between these relativistic quantities and their nonrelativistic counterparts, $\boldsymbol{v} = (d\boldsymbol{r}/dt)$ and $\boldsymbol{a} = (d\boldsymbol{v}/dt)$, is that the rate of change is with respect to proper time instead of time. Let us now see how these relativistic quantities are related to their corresponding nonrelativistic quantities. Toward this end, we define the ratio of the time increment and the proper time increment as the Lorentz factor $\gamma = (dt/d\tau)$. From Eq. (1), $\gamma = 1/\sqrt{1 - (v/c)^2}$, where $v = \sqrt{\boldsymbol{v} \cdot \boldsymbol{v}}$ is the magnitude of the nonrelativistic velocity vector $\boldsymbol{v}$. It follows by differentiation that the relativistic velocity vector and the relativistic acceleration vector in Eq. (2) are related to their nonrelativistic counterparts by

$$\boldsymbol{v}_R = \gamma \boldsymbol{v} \tag{3a}$$

$$\boldsymbol{a}_R = \gamma^2 \left(\boldsymbol{a} + \frac{\gamma^2}{c^2} (\boldsymbol{a} \cdot \boldsymbol{v}) \boldsymbol{v} \right) \tag{3b}$$

where $\boldsymbol{a} \cdot \boldsymbol{v} = a_1 v_1 + a_2 v_2 + a_3 v_3$. Clearly, $\gamma \cong 1$ when $v \ll c$, which corresponds to the nonrelativistic case. It also follows that the relativistic velocity vector and the relativistic acceleration vector in Eq. (3) reduce to their nonrelativistic counterparts when $v \ll c$.

III. Relativity Triangle

We now develop a geometric interpretation of the relativistic acceleration vector in relation to the nonrelativistic acceleration vector. The geometric interpretation has some value in that it further assists the mission planner in understanding relativistic acceleration and in assessing the bending of the trajectory of a spacecraft when it passes by a gravitational source. Equation (3b) gives the relativistic acceleration vector in terms of nonrelativistic quantities: the non-relativistic velocity vector and the nonrelativistic acceleration vector. One obtains the inverse relationship by first recognizing from Eq. (3b) that $\boldsymbol{v} \cdot \boldsymbol{a} = (1/\gamma^4)(\boldsymbol{v} \cdot \boldsymbol{a}_R)$. Substituting this back into Eq. (3b) and solving for $\boldsymbol{a}$

$$\boldsymbol{a} = \frac{1}{\gamma^2} \left[\boldsymbol{a}_R - \frac{1}{c^2} (\boldsymbol{v} \cdot \boldsymbol{a}_R) \boldsymbol{v} \right] \tag{4}$$

Given that the nonrelativistic acceleration vector is a linear combination of the relativistic acceleration vector and the velocity vector, it follows at any given instant of time that the nonrelativistic acceleration vector, the velocity vector, and the relativistic acceleration vector lie in one plane. Without any loss of generality, we shall refer to it as the x–y plane, let the velocity vector act in the x direction, and then rewrite the nonrelativistic acceleration vector as

$$\begin{pmatrix} a_x \\ a_y \end{pmatrix} = \left(1 - \left(\frac{v}{c} \right)^2 \right) \left\{ \begin{pmatrix} a_{Rx} \\ a_{Ry} \end{pmatrix} - \frac{1}{c^2} \begin{pmatrix} v \\ 0 \end{pmatrix} \left[\begin{pmatrix} v \\ 0 \end{pmatrix} \cdot \begin{pmatrix} a_{Rx} \\ a_{Ry} \end{pmatrix} \right] \right\} \tag{5}$$

Next, we express the nonrelativistic acceleration vector and the relativistic acceleration vector as magnitudes multiplied by unit vectors as

$$\begin{pmatrix} a_x \\ a_y \end{pmatrix} = a \begin{pmatrix} \cos(\psi) \\ \sin(\psi) \end{pmatrix}, \quad \begin{pmatrix} a_{Rx} \\ a_{Ry} \end{pmatrix} = a_R \begin{pmatrix} \cos(\psi_R) \\ \sin(\psi_R) \end{pmatrix}$$

where $a = (a_x^2 + a_y^2)^{1/2}$, $a_R = (a_{Rx}^2 + a_{Ry}^2)^{1/2}$, ψ_R is the angle from the velocity vector to the relativistic acceleration vector, and ψ is the angle from the velocity vector to the nonrelativistic acceleration vector, as shown in Fig. 1. Substitute these expressions into Eq. (5) to get

$$a \begin{pmatrix} \cos(\psi) \\ \sin(\psi) \end{pmatrix} = \left(1 - \left(\frac{v}{c} \right)^2 \right) \left\{ -\frac{1}{c^2} a_R v \cos(\psi_R) \begin{pmatrix} v \\ 0 \end{pmatrix} \right.$$
$$\left. + a_R \begin{pmatrix} \cos(\psi_R) \\ \sin(\psi_R) \end{pmatrix} \right\}$$

Finally, dividing by $1 - (v/c)^2$ and rearranging terms yield

$$\begin{pmatrix} \cos(\psi_R) \\ \sin(\psi_R) \end{pmatrix} = \left(\frac{v}{c} \right)^2 \cos(\psi_R) \begin{pmatrix} 1 \\ 0 \end{pmatrix} + \frac{a}{a_R (1 - (v/c)^2)} \begin{pmatrix} \cos(\psi) \\ \sin(\psi) \end{pmatrix} \tag{6}$$

Equation (6) expresses the unit vector that aligns with the relativistic acceleration vector as the sum of a vector of magnitude $(v/c)^2 \cos(\psi_R)$ that aligns with the velocity vector and a vector that aligns with the nonrelativistic acceleration vector. The triangles shown in Fig. 1 give the geometric interpretation of Eq. (6).

First, consider the top triangle. Imagine that spacecraft b is located at the bottom left vertex at an instant of time. Next, at that instant of time, imagine that a source (not shown) is located at some point along
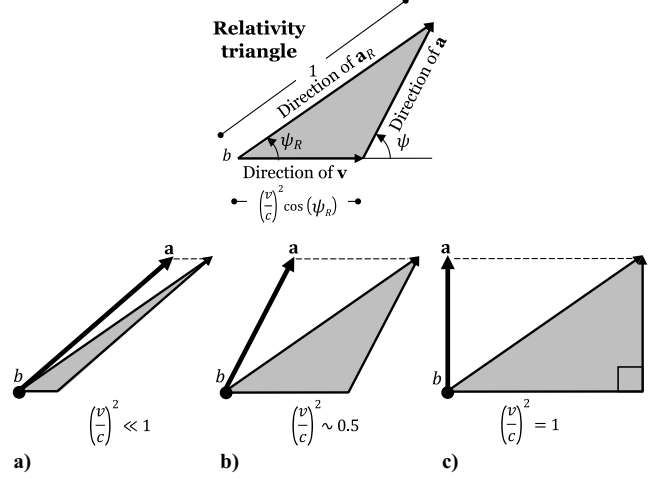

Fig. 1   Relativity triangle.

the line that passes through the bottom left vertex and the top vertex. One might imagine that the source is the sun. The field of the sun produces a force vector $\boldsymbol{F}$ that acts on the spacecraft directed along that line. Furthermore, from the relativistic version of Newton's second law $\boldsymbol{F} = m\boldsymbol{a}_R$ (line 4 of Table 1), we know that the relativistic acceleration vector $\boldsymbol{a}_R$ of the spacecraft is directed along that line, too. The base of the triangle is along the line of the spacecraft's velocity vector $\boldsymbol{v}$. Notice that the base's length varies from 0 when $v = 0$ to $\cos(\psi_R)$ when $v = c$. Finally, the right line is along the line of the spacecraft's nonrelativistic acceleration vector $\boldsymbol{a}$.

Figures 1a–1c depict this situation over a range of speeds. The bottom left vertices of the three triangles correspond to the spacecraft, represented by dots moving to the right at low, medium, and high speeds. The sun (still not shown) is located at an arbitrary point along the line that passes through the line of $\boldsymbol{a}_R$. In Fig. 1a, the spacecraft moves slowly compared to the speed of light. As shown, $\boldsymbol{a}$ and $\boldsymbol{a}_R$ are almost aligned. Figure 1b shows an intermediate case. In Fig. 1c, the speed of the spacecraft is equal to the speed of light. As shown, $\boldsymbol{a}$ and $\boldsymbol{v}$ are perpendicular.

From Eq. (3), we also find that

$$\tan(\psi) = \frac{1}{1 - (v/c)^2} \tan(\psi_R) \tag{7}$$

In Eq. (7), we see that the nonrelativistic acceleration angle ψ depends only on the relativistic acceleration angle ψ_R and the spacecraft's speed v. Figure 2 shows the nonrelativistic acceleration angle ψ as a function of v/c for different relativistic acceleration angles: $\psi_R = 0, 15, 30, 45, 60, 75$, and 90 deg. Notice that the nonrelativistic acceleration angle at $v = 0$ is equal to the relativistic acceleration angle, and that the nonrelativistic acceleration angle increases with v until it reaches 90 deg when $v = c$.

The relativity triangle describes the kinematic behavior of the spacecraft. We see that its nonrelativistic acceleration vector $\boldsymbol{a}$ rotates until it becomes perpendicular to its velocity vector $\boldsymbol{v}$ as the speed v reaches the light limit. This prevents the spacecraft's speed from exceeding the light limit. But, importantly, the acceleration is not zero at the light limit, which is responsible for allowing the spacecraft's trajectory to bend even as the speed approaches the light limit.

We now turn to the governing equations that we will later use to solve four relativistic orbital mechanics problems.

IV. Governing Equations

Over the course of history, two observations of physical behavior have withstood the test of time as transcending circumstance and grew into foundational principles: the principle of light and the principle of impetus. The principle of light, which is a kinematic principle, was described briefly in Sec. II. The principle of impetus is a kinetic principle. It is the intuitive idea that a body's movement, in
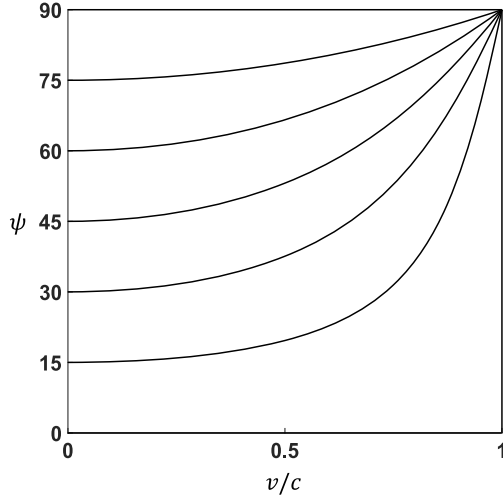
Fig. 2 Nonrelativistic acceleration angle ψ vs v/c for different relativistic acceleration angles: $\psi_R = 0, 15, 30, 45, 60, 75$, and 90 deg.

the absence of influences from other bodies, is constant over time in both magnitude and direction. In NT, the influences referred to in the principle of impetus are forces that are expressed mathematically by $F = ma$, and in SR and SI the forces are expressed mathematically by $F = ma_R$. The interpretation of impetus in NT does not account for the principle of light; for sufficiently large forces, it erroneously predicts speeds that exceed c. The interpretation of impetus in SR only partially accounts for the principle of light; it does not account for the bending of the trajectory of a body when passing by a gravitational source. In fact, in Eddington's famous experiment measuring light bending around the surface of the sun, the prediction in NT is half of the observed value, while in SR the prediction is that there is no light bending at all. General relativity overcame these limitations by introducing the concept of curved spacetime, wherein gravity dictates spacetime's curvature. In GR, the curvature of spacetime produced the influence that changes a body's or light's movement instead of a force producing the influence.

Historically, the modeling of gravitational influence through a curvature of spacetime instead of through a gravitational force, along with the inability of SR to correctly account for the principle of light with a gravitational force, suggested that the concept of gravitational force might be deficient at relativistic speeds but no definitive answer was known one way or the other. With different curved spacetime coordinate systems, it was shown that the singularity at the Schwarzschild radius that appears in his general relativity solution [25] could be removed [26–29]. This raised the question of the "physical" interpretation of the singularity and more generally the possibility that spacetime is not necessarily curved. Other theoretical connections between curved spacetime and ordinary spacetime arose

[23,24]. They, too, left open the possibility that the deficiency in the gravitational force at relativistic speeds might be correctable. The Einstein–Infeld–Hoffman equations produced a relativistic gravitational force from GR under the assumption of a so-called post-Newtonian expansion that is valid for bodies traveling at speeds that are small compared to the speed of light [19]. More recently, Ziefle applied gravitons in a Newtonian framework to approximate gravitational forces for different two-body problems, expressed as $F = G_S Mm/r^2$ in which G_S is a variable gravitational constant. With gravitons, he reproduced the well-known result that $G_S = 2G$ in agreement with GR for a photon passing by a gravitational source and found that $G_S = (1 + \pi(v/c)^2)G$ for the anomalous precession of Mercury [20]. In 2020, the authors of this paper introduced a relativistic correction to the universal law of gravitation for the two-body problem, whose solution agreed numerically with the Schwarzschild solution out to at least three decimal places [21] and in 2021 introduced the Theory of SI [17]. In Appendix A, we give a detailed mathematical proof that the SI solution to the two-body problem is identical to the GR solution discovered by Schwarzschild, confirming that the numerical results earlier obtained were exact.

In the two-body problem, we consider a plane containing a stationary gravitational source of mass M and another body of mass m traveling by the gravitational source. The relativistic universal law of gravitation and the relativistic principle of impetus that SI introduces are

$$F = -\left(1 + 3\left(\frac{v_{R\phi}}{c}\right)^2\right)\frac{GMm}{r^3}r \qquad (8a)$$

$$F = ma_R \qquad (8b)$$

In Eq. (8), $r = (x, y)$ is the position vector from the gravitational source to the mass center of the spacecraft, and $r = |r|$ is distance. The term $1 + 3(v_{R\phi}/c)^2$ is the relativistic correction to the "nonrelativistic" universal law of gravitation, in which $v_{R\phi} = (1/r)(-v_{Rx}y + v_{Ry}x)$ is the azimuthal component of the spacecraft mass center's relativistic velocity vector v_R. Note that the azimuthal component $v_{R\phi}$ of the relativistic velocity vector can be expressed as a radially dependent function using the system's angular momentum. The end of Sec. 2 in Appendix A shows this. Appendix A also proves the full agreement of SI and GR. The SI governing equations that we will apply in this paper are given in Table 1.

Table 1 gives the equations that we will need and makes it clear how the governing equations apply to SI, SR, and NT. As shown, the SR formulation employs lines 3 to 5 but did not treat the influence of a gravitational source (lines 1 and 2). Spacetime impetus employs lines 3 to 5, too, plus it introduces the new relativistic universal law of gravitation (lines 1 and 2). The relativistic potential energy of the gravitational source in SI differs from the nonrelativistic potential energy in NT by the relativistic correction $a(r) = 1 + (v_{R\phi}/c)^2$. The relativistic correction for the gravitational force in line 2 is

Table 1   Governing relationships

	Quantity	Mathematical expression	SI	SR	NT[a]
1	Relativistic potential energy	$V = -\frac{GMm}{r}\left(1 + \left(\frac{v_{R\phi}}{c}\right)^2\right),$ $v_{R\phi} = \frac{\gamma}{r}(-v_x y + v_y x)$ $\gamma = 1/\sqrt{(1 - (v/c)^2}$	✓	✗	✓
2	Gravitational force vector	$F = -\frac{GMm}{r^3}r\left(1 + 3\left(\frac{v_{R\phi}}{c}\right)^2\right)$	✓	✗	✓
3	Relativistic kinetic energy	$T = \frac{1}{2}mv_R^2$	✓	✓	✓
4	Impetus	$F = ma_R$	✓	✓	✓
5	Nonrelativistic acceleration	$a = \frac{1}{\gamma^2}\left[a_R - \frac{1}{c^2}(v \cdot a_R)v\right]$	✓	✓	✓

[a]NT invokes the given quantities without its relativistic terms.

$b(r) = 1 + 3(v_{R\phi}/c)^2$. The relativistic law of impetus $F = ma_R$, which both SI and SR employ, differs from the law of impetus employed by NT that uses the nonrelativistic acceleration vector. In Table 1, The Newtonian theory employs all of the expressions as SI does but is missing the nonrelativistic parts because it does not invoke the principle of light.

V. Relativistic Orbital Mechanics

We are now ready to examine the problem of a spacecraft passing by a stationary gravitational source at a relativistic speed, with a focus on interstellar travel. When are the changes in the speed and/or direction of a spacecraft as it passes by a gravitational source significant? What are the accelerations acting on the spacecraft during a turn? At what distances from a gravitational source are the effects on an interstellar spacecraft negligible, and at what distances could an interstellar spacecraft be captured by a star? As it pertains to telecommunications, what levels of light bending can one expect? Indeed, we will also demonstrate that our formulation treats light bending, too.

For the purposes of interstellar travel, we will consider spacecraft traveling at speeds between $0.1c$ and $0.2c$ and light traveling at c. Also, we will consider analytical and numerical approaches. These problems can be cast in the form of just one general problem. The general problem is of a body, a spacecraft or a photon of light, that is initially located at point a, a distance R from a stationary gravitational source, and initially traveling at speed v at turn angle θ relative to the line between the body and the source. The perpendicular distant $B = R\sin(\theta)$ is called the impact parameter. The impact parameter is 0 when the body is initially traveling in the radial direction. When solving this problem analytically, we can additionally construct a circle of radius r around the source. At some point in the motion, the body may intersect that circle at entry point b. At entry point b, we will be able to determine analytically the entry speed v_b of the body and the entry angle α that the trajectory makes relative to the tangent of the circle (see Fig. 3).

The radius of the circle is arbitrary; we could set it to a value that is very close or far from the source. The analytical procedure for finding the entry speed v_b and the angle α is outlined in Table 2.

The procedure draws on conservation of relativistic energy and relativistic angular momentum about the source point. Column 1 gives the needed expressions from which column 2 solves for an unknown evaluated at point b in the expression to the left of it. Line 1
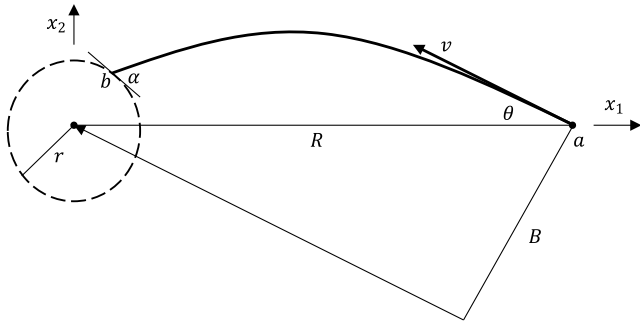
of column 1 gives the two governing relativistic conservation equations from which line 1 of column 2 determines the kinetic energy at point b, recognizing that $E = T + V$ for the T and V given in Table 1. Line 2 of column 1 gives the relativistic kinetic energy from which line 2 of column 2 determines the speed at b. Line 3 of column 1 gives the relativistic angular momentum from which line 3 of column 2 determines the azimuthal component of velocity $v_{b\phi}$ at point b. Finally, we determine the entry angle α from $\cos\alpha = v_{b\phi}/v_b$. These analytical solutions are not complete; they do not determine the location of entry point b. One must determine the location of entry point b by numerically integrating the nonrelativistic acceleration to find the full trajectory. Appendix B gives a case study that shows how to solve this general problem numerically.

Next, we solve four illustrative problems.

A. Relativistic Gravitational Flyby of a Spacecraft

We begin by considering the relativistic gravitational flyby of a spacecraft as it passes by Alpha Centauri A. Alpha Centauri A's mass is $M_A = 1.1M$, where M is the sun's mass. Its radius is $R_A = 1.22R_S$, where the sun's radius is R_S (see Table 3).

Figure 4 shows a typical relativistic flyby. As shown, the spacecraft is initially located at $(x_1(0), x_2(0))$, where its speed is $v(0)$ to the left. After a time t_f, the turn or trajectory angle becomes $\theta_f = \theta(t_f)$. The results are given in Table 4 for the nine cases we examined. The results were obtained by numerically integrating the expression for the nonrelativistic acceleration vector in Table 1; see Appendix B for a tutorial on the solution steps. In each case, the spacecraft is initially $20R_A$ from the source in the x_1 direction. For cases 1 and 2, the initial speed is $0.2c$ and the lateral offsets in the x_2 direction are $20R_A$ and $10R_A$, respectively. For cases 3 to 9 the lateral offset is $5R_A$ and the initial speeds range from $0.001c$ to $0.7c$. We determined for each case the angles θ_f that the spacecraft turns as predicted by SI and SR and the error and percentage error between them. Note that because SI and GR transform to the same governing equations (Appendix A), the SI

Table 3   Sun and Alpha Centauri A data

		Sun	Alpha Centauri A
Mass	M	1.989×10^{30} kg	M_A 2.188×10^{30} kg
Radius	R_S	696,000,000 m	R_A 849,120,000 m
Schwarzschild radius	r_S	2,970 m	r_A 3,267 m
	Other		
Universal gravitational constant	G	6.674×10^{-11} m^3/kg · s^2	
Speed of light	c	2.99×10^8 m/s	

Fig. 3   General problem setup.

Table 2   Angular momentum and energy

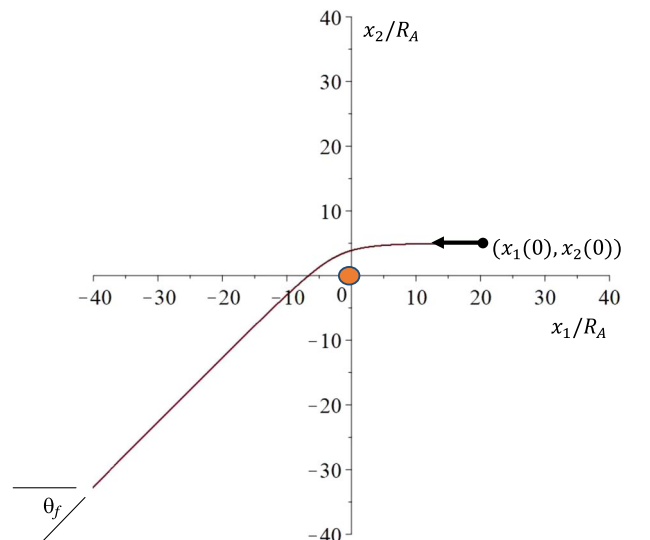|	1	2
1	$H_a = H_b, E_a = E_b$	$T_b = T_a + V_a - V_b$
2	$T = \dfrac{\frac{1}{2}mv^2}{1-(v/c)^2}$	$v_b = c\sqrt{\dfrac{2T_b}{mc^2 + 2T_b}}$
3	$H = \dfrac{mrv_\phi}{\sqrt{1-(v/c)^2}}$	$v_{b\phi} = \dfrac{H_b}{mr_b}\sqrt{1-(v_b/c)^2}$ $\cos\alpha = v_{b\phi}/v_b$

Fig. 4   Spacecraft passes by Alpha Centauri A.

Table 4   Turn angle for SI and SR

	$x_2(0)$	v/c	t_f, s	$\theta(t_f)$ (SI),[a] deg	$\theta(t_f)$ (SR), deg	$\Delta\theta$, deg	Difference, %
1	$20R_A$	0.2	3,000	2.458157×10^{-4}	2.250536×10^{-4}	2.076×10^{-5}	8.5
2	$10R_A$	0.2	3,000	5.444575×10^{-4}	5.007283×10^{-4}	4.373×10^{-5}	8.0
3	$5R_A$	0.001	300,000	45.424094	45.423908	1.863×10^{-4}	<0.00
4	$5R_A$	0.01	30,000	4.343358×10^{-1}	4.342469×10^{-1}	8.883×10^{-5}	0.02
5	$5R_A$	0.1	3,000	4.383648×10^{-3}	4.383648×10^{-3}	8.812×10^{-5}	2.0
6	$5R_A$	0.2	1,500	1.129445×10^{-3}	1.041333×10^{-3}	8.811×10^{-5}	7.8
7	$5R_A$	0.3	900	5.267065×10^{-4}	4.385956×10^{-4}	8.811×10^{-5}	16.7
8	$5R_A$	0.5	500	2.182122×10^{-4}	1.301010×10^{-4}	8.811×10^{-5}	40.4
9	$5R_A$	0.7	400	1.333080×10^{-4}	4.515249×10^{-5}	8.799×10^{-5}	66.0

[a]The results in this column agree with GR.

results agree exactly with the GR results (column 4 in Table 4). As a numerical check, we verified this agreement, although it was unnecessary to explicitly include the GR results in the tables and figures. The closest approach to Alpha Centauri A in the problems treated as follows is about $5R_A$, which for reference is close to half of the Parker probe's closest approach to the sun of about $9.8R_S$ (see Appendix B). In case 1, the error $\Delta\theta$ in the SR prediction of the turn angle θ_f is the smallest among the cases treated; it is about 0.00002 deg. Although very small, it quickly results in large errors in lateral directions relative to the SR predictions. In case 1, the spacecraft is initially traveling at $0.2c$, and so 5 s after passing Alpha Centauri A, the SR error results in a lateral error of $D\Delta\theta \cong 7$ km, where D is distance of travel. In a return-to-Earth scenario, the lateral error would become $D\Delta\theta \cong 15$ AU, which is about the span of our solar system.

For cases 3 through 9, Fig. 5 shows a log–log plot of the turn angles θ_f vs v/c. In the log–log plot, the relationship is close to linear, which corresponds to a nearly inverse-square dependence (slope of -2) between the turn angle and v/c.
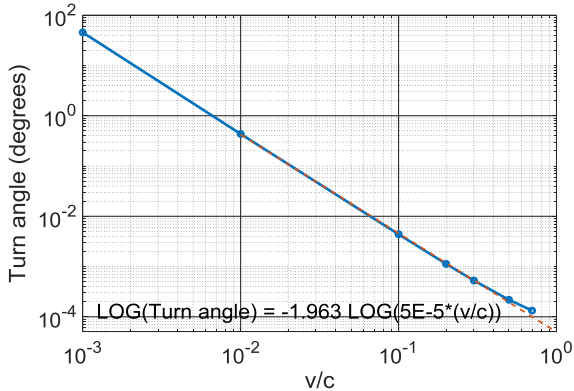
Fig. 5   Turn angle vs v/c (SI cases 3 to 9).

Next, we examine the relativistic accelerations during the turns. Per line 4 in Table 1, the gravitational force on the spacecraft is equal to the spacecraft's mass multiplied by its relativistic acceleration. The relativistic accelerations predicted by SI and SR are given in Table 5 for the same previously considered cases 1 through 9.

Notice that the relativistic accelerations are given in Earth g's (9.8 m/s^2). Cases 1 and 2 fly by the source at the largest distances from the source from among the cases considered, and their peak g's are the smallest (on the order of 5–20%). The peak g's in cases 3 through 9 differ by their initial speeds. The cases increase in initial speed to $0.7c$, and their g's increase from about 1.5 to 3.2. Notice from case 3 to case 4 that there is a dip in the g's. One expects this dip because of two competing trends. When the initial speed is sufficiently small, the trajectory will turn toward the source and experience a high peak acceleration when passing by the source. On the other hand, when the initial speed becomes sufficiently high, the least distance between the source and the spacecraft approaches the initial offset, at which point further increases in speed cause a corresponding increase in g's. We also see this in the log–log plot of the turn angle (Fig. 5), which shows that the turn angle decreases in an almost inverse square proportion to speed. Finally, note that the dynamic stresses that act on the vehicle when it passes a gravitational source are not proportional to the accelerations and resulting peak loading; dynamic stresses result from the gravity gradients, which are considerably smaller.

B.   Relativistic Circular Orbits of a Spacecraft

In this problem, we determine the speeds of a family of circular orbits of a spacecraft around a stationary gravitational source. The family of circular orbits gives a general sense of the relationship between the radius and the speed of an orbit. The Newtonian theory and SR predict that there is no limit to how small the radius of a stable circular orbit can be; both differ from general relativistic mechanics (SI and GR), which predict the well-known nonzero lower limit radius of a circular orbit, below which a circular orbit is unstable.

Table 5   Peak relativistic accelerations (in Earth g's) for SI and SR

	$x_2(0)$	v/c	t_f, s	$a_{R\max}/g$ (SI)[a]	$a_{R\max}/g$ (SR)	$\Delta a_{R\max}/g$	Difference, %
1	$20R_A$	0.2	3,000	0.058	0.052	0.006	10.3
2	$10R_A$	0.2	3,000	0.232	0.207	0.025	10.8
3	$5R_A$	0.001	300,000	1.541	1.541	1.1×10^{-5}	0.0
4	$5R_A$	0.01	30,000	0.832	0.832	2.5×10^{-4}	0.0
5	$5R_A$	0.1	3,000	0.852	0.827	0.025	2.9
6	$5R_A$	0.2	1,500	0.930	0.827	0.103	11.1
7	$5R_A$	0.3	900	1.072	0.827	0.245	22.9
8	$5R_A$	0.5	500	1.653	0.827	0.827	50.0
9	$5R_A$	0.7	400	3.209	0.826	2.383	74.3

[a]The results in this column agree with GR.

Table 6 Velocity calculations for circular orbits

Line 1

SI (and SR for $b = 1$)	NT

$$\boldsymbol{F}_a = \begin{pmatrix} F_r \\ F_\phi \end{pmatrix} = -\frac{GMm}{r^3} b(r) \begin{pmatrix} r \\ 0 \end{pmatrix} = m \begin{pmatrix} a_{Rr} \\ a_{R\phi} \end{pmatrix} \qquad \boldsymbol{F}_a = \begin{pmatrix} F_r \\ F_\phi \end{pmatrix} = -\frac{GMm}{r^3} \begin{pmatrix} r \\ 0 \end{pmatrix}$$

$$\boldsymbol{a}_a = \begin{pmatrix} \ddot{r} - r\dot\phi^2 \\ r\ddot\phi + 2\dot{r}\dot\phi \end{pmatrix} = \begin{pmatrix} -r\dot\phi^2 \\ 0 \end{pmatrix} \qquad \boldsymbol{a}_a = \begin{pmatrix} \ddot{r} - r\dot\phi^2 \\ r\ddot\phi + 2\dot{r}\dot\phi \end{pmatrix}$$

$$= \frac{1}{\gamma^2}\begin{bmatrix} 1 - (v_r/c)^2 & -(v_r/c)(v_\phi/c) \\ -(v_r/c)(v_\phi/c) & 1 - (v_\phi/c)^2 \end{bmatrix}\begin{pmatrix} a_{Rr} \\ a_{R\phi} \end{pmatrix} \qquad = \begin{pmatrix} -r\dot\phi^2 \\ 0 \end{pmatrix} = \frac{1}{m}\begin{pmatrix} F_r \\ F_\phi \end{pmatrix}$$

Line 2

SI	NT

$$-r\dot\phi^2 = -\frac{GMr}{r^3}\left(1 - \left(\frac{r\dot\phi}{c}\right)^2 + 3\left(\frac{mr^2\dot\phi}{mc}\right)^2\frac{1}{r^2}\right) \qquad -r\dot\phi^2 = -\frac{GMr}{r^3}$$

Line 3

SR (SI for $b = 1$)

$$r\dot\phi^2 = -\frac{GMr}{r^3}\left(1 - \left(\frac{r\dot\phi}{c}\right)^2\right)$$

Line 4

SI	SR (SI for $b = 1$)	NT

$$\frac{v_\phi}{c} = \sqrt{\frac{1}{2}\left(\frac{\frac{r_s}{r}}{1 - \frac{r_s}{r}}\right)} \qquad\qquad \frac{v_\phi}{c} = \sqrt{\frac{\frac{r_s}{r}}{2 + \frac{r_s}{r}}} \qquad\qquad \frac{v_\phi}{c} = \sqrt{\frac{1}{2}\left(\frac{r_s}{r}\right)}$$

Table 7 Five circular orbits

	$\frac{v_\phi}{c}$	$\left(\frac{r}{r_s}\right)^{SI}$	$\left(\frac{r}{r_s}\right)^{SR}$	$\left(\frac{r}{r_s}\right)^{NT}$
1	1	1.5	0	0.5
2	0.5	3	1.5	2
3	0.2	13.5	12	12.5
4	0.1	51	49.5	50
5	0.01	5001	4999.5	5000

Table 8 Relativistic gravitational entry

| Parameters	Values
r	R_A
R	$5R_A$
v_a	$0.001c$
θ	20 deg
v_b	$0.002c$
α	32.1 deg

For the purposes of comparison and general interest, Table 6 gives the development of the NT, SR, and SI solutions.

Line 1 gives the gravitational force vector and the nonrelativistic accelerations for SI, SR, and NT. Line 2 determines $r\dot\phi^2$ from line 1 for SI and NT, and line 3 determines $r\dot\phi^2$ from line 1 for SR. Line 4 determines the circular-orbit tangential velocity (speed) for SI, SR, and NT in terms of the Schwarzschild radius $r_s = (2GM/c^2)$. Here, it is interesting to glimpse where the Schwarzschild radius singularity $1 - (r_s/r)$ first appears in SI. In SI, it first appears in line 4, and in GR it is found in the Schwarzschild metric itself. Table 7 shows the predictions by SI, SR, and NT for five noteworthy cases.

The SI solution in case 1 is the radius $r = 1.5r_s$ of the well-known photon sphere predicted by GR. As shown, SR predicts a circular orbit only at the origin for a speed of c, while NT predicts a circular orbit at $r = 0.5r_s$ at the speed c of light. Of course, only one of these results can be correct, and that result is predicted by SI in agreement with GR. The SI solution in case 2 is the well-known transition radius below which a circular orbit is unstable and above which the circular orbit is stable [22]. Cases 3 and 4 correspond to a range of speeds that many believe will be typical of interstellar cruise. Case 5 is sufficiently slow that the relativistic correction is in the fourth significant figure.

C. Relativistic Gravitational Orbital Insertion

We now consider a spacecraft that is inserted into an orbit, in particular, an example in which the spacecraft crashes into Alpha Centauri A's surface (using the term "surface" only loosely). Referring to Fig. 3, we set the initial position to $(5R_A, 0)$ with an initial speed of $v_a = 0.001c$ at an angle of $\theta = 20$ deg, and we let $r = R_A$ (Table 8). We numerically solve this problem from the SI governing equations in line 4 of Table 1 by expressing the nonrelativistic acceleration in line 5 in terms of the relativistic gravitational force in line 2. We also analytically solve this problem to find the entry velocity and angle by following the procedure that Table 2 outlines. Of course,
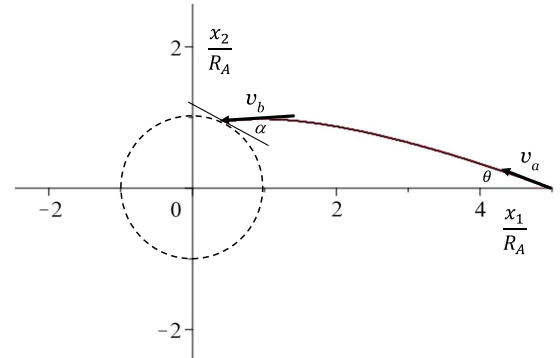
Fig. 6 Relativistic gravitational entry.

both methods produce the same results. When reaching the surface, we determined that the spacecraft's speed is $0.002c$, where its entry angle is 32.1 deg (Table 8; Fig. 6). Initially, the nonrelativistic acceleration angle and the relativistic acceleration angle were $\psi = 20$ deg and $\psi_R = 20$ deg, respectively (no difference in the second significant figure). When reaching the surface of Alpha Centauri A, they were $\psi = 57.5$ deg and $\psi_R = 57.3$ deg, respectively. Because of the speed being small in comparison to c, its doubling during the approach caused only a slight increase in the difference between the nonrelativistic and relativistic acceleration angles. More generally, the spacecraft only reaches relativistic speeds when its proximity to the center of the source approaches the Schwarzschild radius.

D. Grazing of Light Past a Gravitational Body

The problem of light grazing is identical to the spacecraft problem of a relativistic flyby, the difference being in the orders of magnitude of the speeds. Both problems employ the same equations. The mass of

Table 9   Turn angle for SI and SR approaching the speed of light

	$x_2(0)$	v/c	t_f, s	$\theta(t_f)$ (SI),[a] deg	$\theta(t_f)$ (SR), deg	$\Delta\theta$, deg	Difference, %
1	$5R_A$	0.999	600	8.825288×10^{-5}	8.794143×10^{-8}	8.804×10^{-5}	99.8
2	$5R_A$	0.9999	600	8.817372×10^{-5}	8.782275×10^{-9}	8.804×10^{-5}	100
3	$5R_A$	0.99999	600	8.816582×10^{-5}	8.781090×10^{-10}	8.816×10^{-5}	100
4	$1R_A$	0.9999	600	4.408905×10^{-4}	4.408374×10^{-8}	4.402×10^{-4}	100
5	$1R_A$	0.99999	600	4.408508×10^{-4}	4.407779×10^{-9}	4.408×10^{-4}	100
6	$1R_A$	0.999999	600	4.408468×10^{-4}	4.407720×10^{-10}	4.408×10^{-4}	100

[a]The results in this column agree with GR.

Table 10   Peak relativistic acceleration (in Earth g's) for SI and SR

	$x_2(0)$	v/c	t_f, s	$a_{R\max}/g$ (SI)[a]	$a_{R\max}/g$ (SR)	$\Delta a_{R\max}/g$	Difference, %
1	$5R_A$	0.999	600	1,239	0.8	1,238	99.9
2	$5R_A$	0.9999	600	12,398	0.8	12,397	100
3	$5R_A$	0.99999	600	123,992	0.8	123,991	100
4	$1R_A$	0.9999	600	3.1×10^5	21	3.1×10^5	100
5	$1R_A$	0.99999	600	3.1×10^6	21	3.1×10^6	100
6	$1R_A$	0.99999	600	3.1×10^7	21	3.1×10^7	100

[a]The results in this column agree with GR.

the light photon is extremely small, but it drops out of the equations, and so this has no effect on the solution. As in the first problem, we shall here again take the source to be Alpha Centauri A. Recall that the parameters were given in Table 3 and that Fig. 4 shows a typical relativistic flyby. Again, we solved the problem both numerically and analytically. The results in Tables 9 and 10 are for the six cases we examined.

In each case, the light photon is initially $40R_A$ from the source in the x_1 direction, laterally offset by $5R_A$ (cases 1 to 3) and by R_A (cases 4 to 6) in the x_2 direction and traveling in the $-x_1$ direction at speeds approaching c. We determined for each case the angles θ_f that the light bends as predicted by SI. Again, because SI and GR transform to the same governing equations (Appendix A), the SI results agree exactly with the GR results and became unnecessary to include in the tables and figures. The initial speeds of the light photons were between $v = 0.999c$ and $0.999999c$. We deliberately chose speeds in this range to find the limiting behavior. Notably, we let v approach c and did not set it equal to c.

We performed cases 1 to 3 and cases 4 to 6 to illustrate convergence to speed c. Notice as the speed approaches c that the SI turn angle is convergent. Because of the equivalence of SI and GR, the turn angle converges to the value determined by the well-known GR bending of light formula, $\delta_N = (4GM/c^2B)$, where B is the impact parameter or distance of closest approach during the orbit. For $v = 0.999999c$ at release point ($40R_A$ $1R_A$), the impact parameter is $1R_A$. The classical formula gives $\delta_N = (4GM/c^2R_A) = 7.694 \times 10^{-6}$ rad $= 4.408 \cdot 10^{-4}$ deg, in agreement with the SI simulation.

We performed cases 4 to 6, again, to converge to a speed of c. Again, from the GR light formula for light grazing the surface of Alpha Centauri A, we get, as expected, $\delta_N = (4GM/c^2R_A) = 4.408 \cdot 10^{-4}$ deg, in agreement with the SI simulations. As shown, the offset in cases 1 to 3 is five times greater than in cases 4 to 6, and the turn angle is five times smaller than in cases 4 to 6. The turn angles, although very small, can have a significant effect over large distances and therefore the return-to-Earth communication signature. Also, notice in the rest frame of reference that SR converges to no bending as the speed approaches c, as expected.

Finally, because light bending and spacecraft turning are mathematically the same problem, it is interesting to note how the relativistic accelerations in light bending change (Table 10). We see as the light speed approaches c that the relativistic accelerations increase rapidly. With each decimal place closer to c, the relativistic g increases by an order of magnitude.

This and the previous three problems are illustrative of the basic relativistic orbital physics that will underlie tradeoff mission design studies, energy and cost budgeting, and astronavigation optimization for interstellar travel.

VI.   Discussion

This paper applied to the problem of interstellar travel of spacecraft, a new relativistic formulation of mechanics that can greatly simplify the predictions. Commensurate with the level of mathematical and physics training that a mission specialist or any other typical aerospace scientist has received, this paper was written for nonexperts in GR. Indeed, the new formulation is called spacetime impetus and is unique because it does not explicitly require GR; its hallmark difference is that it instead employs a relativistic universal law of gravitation.

This paper solved four relativistic orbital mechanics problems: three for spacecraft and one for light. When applying SI, we cast the problems in the form of just one general problem: of a spacecraft or a photon of light that is initially located at point a, a distance R from a stationary gravitational source, and initially traveling at speed v making an angle θ relative to the line between the body and the source (Fig. 3). We considered both analytical and numerical approaches.

The first problem was the relativistic gravitational flyby of a spacecraft as it passes by Alpha Centauri A. We examined the turn angle, how sensitive it is to lateral distance, and we compared it to SR. We observed a significant change in the direction of a spacecraft when it passes by a gravitational source (Table 4). We also examined the accelerations of the spacecraft during the turns (Table 5).

The second problem cataloged a family of circular orbits of a spacecraft. It is a simple way to see the relationship between the radius and speed of an orbit. We also showed how SR and SI compare in the interstellar travel range of $0.1c$ to $0.2c$. We saw that the differences in speed and orbit radius predicted by SR and SI can be quantitatively significant in that range (Table 6).

The third problem examined a spacecraft that undergoes an orbital insertion, in particular a crash into Alpha Centauri A's surface. The spacecraft was not initially traveling at a relativistic speed. We found that it would only reach a relativistic speed when its proximity to the center of the source approaches the Schwarzschild radius.

The fourth and last problem pertained to telecommunications: examining the levels of light bending one can expect. The light

bending problem is identical to the spacecraft problem of relativistic flyby with the exception of the orders of magnitude of the speeds. We examined light grazing Alpha Centauri A and obtained turn angles that are very small but that can have a significant effect over large distances and therefore to the return-to-Earth communication signature.

In addition to these illustrative problems, this paper also developed a geometric interpretation of the relativistic acceleration vector in relation to the nonrelativistic acceleration vector. It can assist the mission planner in the assessment of the bending of a spacecraft trajectory when it passes by a gravitational source.

With respect to the more theoretical aspects of the SI methodology, Appendix A discusses the need for a relativistic universal law of gravitation and demonstrates why it generates the same trajectories that one obtains in GR. A rigorous derivation introduced the mathematical mapping between SI and GR, from which we proved that the SI governing equations and GR governing equations are in full agreement.

A unique feature of the SI analysis is that it retains the concept of force along with its free body diagrams and, derived from this, its impulse–momentum and work–energy principles, over the full range of speeds. This is responsible for it being relatively straightforward to apply.

VII.   Conclusions

Interstellar vehicles will pass by gravitational sources, which will raise navigation and communication issues that must account for general relativistic effects. Indeed, the planning for these missions will require simulation software that performs mission design trade-off studies, energy and cost budgeting, optimization, etc., all of which will have to incorporate these general relativistic effects. Toward this end, this paper applied a new relativistic formulation of mechanics, called spacetime impetus, which was shown to greatly simplify the incorporation of these relativistic effects. Spacetime impetus overcame the limitation of SR not accounting for the presence of a gravitational source, but instead of adopting the GR approach, which relies on a mathematical apparatus for curved spacetime, it keeps SR's spacetime metric and employs a relativistic gravitational force vector, which simplifies many of the difficulties that come from implementing the GR methodology. The analyst can now update nonrelativistic mission planning codes to give them general relativistic capabilities. It requires augmenting the code with relativistic velocities and relativistic accelerations, replacing a non-relativistic universal law of gravitation with a relativistic universal law of gravitation, and setting up Lorentz transformations between frames. Also, Appendix B examines the orbit of the Parker Solar Probe around the sun, serving as a nice tutorial problem for those who seek to program the SI methodology.

Appendix A: Spacetime Impetus: Analytical Verification

A.1.   Background

Many in physics well understand that the connections between the different branches of physics are obscured by the disconnected mathematical foundation upon which they currently rely. It is clear, in the absence of external influences, that light travels along a straight line at a constant speed, just as the particle does. This sense of the state of physics finds considerable support in the physics community, and it motivated the original research that led to the theory of spacetime impetus (SI). The fundamental hypothesis is that the differences purported to exist between the electromagnetic, mechanical, and quantum realms do not result from the differences in our notions about matter as much as from the differences in their states, with electromagnetic and quantum behaviors reflecting miniscule fragments of energy traveling at immense speeds and mechanical behavior reflecting comparatively immense fragments of energy traveling at comparatively miniscule speeds. The argument is made that the particle and the wave are existentially opposite and complementary forms of energy. The particle corresponds to a source of energy surrounded by a void, and the wave corresponds to radiated energy

without regard to the source: incomplete when one is considered in isolation of the other. The idea is that it is better to think of the building block as a fragment of energy, an energy distribution that radiates outward from its source point.

Pertaining to the support in the physics community for the connections between the different branches of physics, when considering the relationships between Newtonian theory (NT), special relativity (SR), and general relativity (GR), the following connections are observed: Connection 1) all three employ a four-dimensional framework, Connection 2) all three employ the principle of impetus, Connection 3) all three are covariant, and Connection 4) SR and GR employ the principle of light. Pertaining to the concept of influence, Connection 5) NT and SR describe influence by an interaction force, and Connection 6) GR by a spacetime curvature vector. Finally, pertaining to GR, it first appears to be the least connected to the other theories because of its employment of a curved spacetime framework, a principle of equivalence, and a principle of least action. However, Connection 7) each of these devices is connected to the devices that the other theories draw from. We now consider each of these connections one at a time:

Connection 1): The Newtonian framework is dictated by the spatial metric $dl^2 = dx_r dx_r$ (summing over r from 1 to 3) and an independent temporal coordinate from which one derives the Galilean transformation. The Minkowski framework is dictated by the spacetime metric $c^2 d\tau^2 = c^2 dt^2 - dl^2$ from which one derives the Lorentz transformation. General relativity employs the Riemannian framework dictated by the curved spacetime metric $c^2 d\tau^2 = g_{rs} dx_r dx_s$ (summing over r and s from 0 to 3) for which the principle of least action leads to the generally covariant governing equation $0 = (d^2 x_t / c^2 d\tau^2) + \Gamma^t_{rs}(dx_r/cd\tau)(dx_s/cd\tau)$ (summing over r and s from 0 to 3), where the affine connection Γ^t_{rs} is defined in terms of the metric coefficients g_{rs} by $\Gamma^t_{rs} = (1/2)g^{tq}((\partial g_{qr}/\partial x_s) + (\partial g_{rs}/\partial x_q) + (\partial g_{sq}/\partial x_r))$ (summing over q from 0 to 3), where $g^{ru}g_{us} = \delta_{rs}$ (summing over u from 0 to 3).

Connection 2): The principle of impetus in the Newtonian framework is $F_r = ma_r (r = 1, 2, 3)$ and in the spacetime framework is $F_r = ma_{Rr}(r = 1, 2, 3)$. The principle of impetus is mathematically equivalent to the principle of least action, and so, in principle, GR employs the principle of impetus, too.

Connection 3): Covariance refers to the notion that governing equations should hold locally across frames of reference. In NT, the existence of an inertial frame was once believed to violate covariance. The Newton–Cartan theory [23] showed that NT is covariant, and covariance was later applied across theories [24].

Connection 4): The Newtonian theory does not apply to light, and SR applies to light except in the presence of a gravitational source.

Connection 5): Spacetime impetus distinguishes between an action force vector $P_r (r = 1, 2, 3)$ and an interaction force vector $F_r (r = 1, 2, 3)$. The action force vector is a field quantity associated with a source. In contrast, the interaction force vector is associated with a source and the body on which it acts. They are related by $F_r = mP_r$, where m is the mass of the body on which the force vector acts. Historically, this distinction was not present in NT, which resulted in some ambiguity and then why inertial mass and gravitational mass were inexplicitly equal [21].

Connection 6): The Newtonian theory describes influence mathematically by the concept of force, applying it to general externally applied cases and in particular to gravitational forces governed by a universal law of gravitation. Special relativity describes influence mathematically by the concept of force, too, applying it to general externally applied forces, but it treated the gravitational force incorrectly. General relativity describes influence mathematically by the curvature of spacetime, where the curvature is produced by gravitation.

Connection 7): These differences are more superficial than substantive. Historically, the principle of equivalence and the principle of least action were invoked to justify replacing the gravitational force with a corresponding curvature of spacetime. These steps produced a geometrized description of physical behavior that is governed by geodesic equations. The geodesic equations express the principle of least action for an action that is set equal to $\int d\tau$. However, it has been

deduced from the existence of a mapping between the Minkowski and Riemannian frameworks and from the equivalence of the principles of least action and of impetus in the Minkowski spacetime framework that the mapping from the Minkowski framework to the Riemannian framework was never necessary, and that one could have started with the principle of impetus, at least for the problem of a body passing by an isotropic gravitational source.

A.2.   Need for a Relativistic Universal Law of Gravitation

Spacetime impetus provided an important connection between NT, SR, and GR. The SI connection to NT stemmed from SI's relativistic correction to the universal law of gravitation employed by NT. The SI connection to SR was made by adopting the spacetime metric employed by SR. Finally, the SI connection to GR arose from SI's governing equations, which transform mathematically to the same equations in GR that govern the motion of a body under the influence of a gravitational source. We now address the steps that motivated the SI connection to NT, specifically the relativistic universal law of gravitation.

To motivate the need for a relativistic universal law of gravitation, we first return to NT and refer to Fig. A1, which shows a body passing by a stationary gravitational source at a speed v. At the instant shown, the source draws the body toward it. In NT, one expresses this attraction by a gravitational force vector F that obeys the universal law of gravitation. NT expresses the concept of impetus by its second law $F = ma$. When the speed of the body is near the light limit, the gravitational force vector together with the second law predict that the body's speed will just continue to increase beyond the light limit, violating the principle of light.

Altogether, there were the following three options to address this violation, recognizing that it stemmed from the employment of the two aforementioned propositions and from not employing a principle of light:

1) Modify the universal law of gravitation in NT.
2) Modify the second law in NT.
3) Replace the universal law of gravitation in NT, the second law in NT, or both.

From among these options, SR sought to satisfy the principle of light by adopting remedy 2, that is, by reformulating the second law in spacetime. It replaced the spatial metric $dl^2 = dr \cdot dr$ with the spacetime metric $c^2 d\tau^2 = c^2 dt^2 - dl^2$ and modified its definition of linear momentum from mv, where m is mass and v is the non-relativistic velocity vector, to mv_R, where v_R is the relativistic velocity vector. These modifications successfully limited the speeds of bodies to that of light and were mathematically consistent with electromagnetism. However, SR did not account for the bending of light or the bending of the path of any other body traveling at a relativistic speed when it passes by a gravitational source. In fact, with the universal law of gravitation, SR incorrectly predicts that the path of light in the presence of a nearby gravitational source does not bend. Thus, the question remained how to correctly predict the bending of the trajectory of a body when it passes by a gravitational source. From among the possible remedies to these problems with NT and SR, GR adopted remedy 3, abandoning remedies 1 and 2, while recognizing that it would need to agree with NT when the speed of the body is small compared to the light limit. The originally adopted approach was to formulate a minimum proper time (least action) problem in a curved spacetime, where its curvature is governed by a Riemannian metric that satisfies the principle of light and the effect of gravity. For the two-body gravitational problem, the Riemannian metric reduces to the Schwarzschild metric. The GR mathematical appar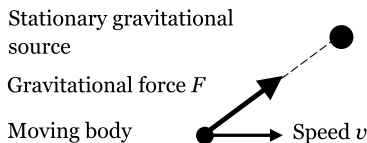atus was formidable; it never became standard fare in education, which continues to make it difficult for the spacecraft and rocketry communities, among others, to analyze the trajectories of bodies that are bent by nearby gravitational sources.

From among the possible remedies to the problems with NT and SR, SI addressed the aforementioned predicament in a very different way. Spacetime impetus adopted remedies 1 and 2, instead of adopting remedy 3. In fact, SI adopted the same remedy 2 that SR adopted, but unlike SR it also adopted remedy 1. It modified the gravitational law so that it conforms to the principle of light.

Toward this end, two important requirements were invoked. First, it can be shown that the gravitational force vector, to conform to the principle of light, must satisfy proper limiting conditions; it would need to be on the order of γ^2. (The eigenvalue problem for the transformation from relativistic acceleration components to nonrelativistic acceleration components developed in [17] gives the necessary limiting conditions.) Second, it was understood that the lack of bending in SR is not an affliction for the radial component of the trajectory because it already points toward the source and has no need to bend. The affliction results from the component perpendicular to the radial direction in the plane of the two-body problem (the azimuthal direction). Thus, the SI development singled out a factor of the form

$$\frac{1 - \left(\frac{v_r}{c}\right)^2}{1 - \left(\frac{v}{c}\right)^2} = 1 + \frac{\left(\frac{v_\phi}{c}\right)^2}{1 - \left(\frac{v}{c}\right)^2} = 1 + \left(\frac{v_{R\phi}}{c}\right)^2$$

As required, this factor, when multiplied by the gravitational potential energy in NT, is on the order of γ^2 and is such that it does not affect the radial component of the body's motion. The relativistic potential energy (fragment of energy) takes on the form

$$V = -\left(1 + \left(\frac{v_{R\phi}}{c}\right)^2\right)\frac{GMm}{r}, \quad a(r) = 1 + \left(\frac{v_{R\phi}}{c}\right)^2$$

where $a(r)$ is the relativistic correction in the potential energy. (The fragment of energy refers to the potential energy of a point source of energy.) Taking partial derivatives with respect to the spatial coordinates, we obtain the relativistic universal gravitational law

$$F_r = \left(1 + 3\left(\frac{v_{R\phi}}{c}\right)^2\right)\frac{GMm}{r^3}x_r \qquad b(r) = 1 + 3\left(\frac{v_{R\phi}}{c}\right)^2$$

where $b(r)$ is the relativistic correction in the force vector. [One finds the gravitational force vector from $F = -\nabla V$. When taking partial derivatives, the term $v_{R\phi}$ appears to be an explicit function of time. However, from conservation of relativistic angular momentum, one can express $v_{R\phi}$ as an explicit function of r. The angular momentum of the two-body system about the system's mass center is $H = r\mu v_{R\phi}$, where $\mu = Mm/(M + m)$ is the reduced mass, and so $v_{R\phi} = H/(r\mu)$. Upon substitution, one can then take the needed partial derivatives. Also, note for spacecraft that $m \ll M$ for which it is sufficient to set μ equal to m].

A.3   Relativistic Universal Law of Gravitation and the Schwarzschild Solution: A Mathematical Proof

In the following, we first set up the mathematics of ordinary spacetime, state the propositions made by SI and GR, describe the structure of the proof, and then develop the temporal map and the spatial map that prove that the SI solution and the Schwarzschild solution are identical.

a.   Ordinary Spacetime

We first set up the ordinary spacetime framework according to which

$$c^2 d\tau^2 = c^2 dt^2 - dl^2 \qquad (A1a)$$

Stationary gravitational source

Gravitational force F

Moving body   Speed v

Fig. A1   Body passing a gravitational source.

$$dl^2 = d\boldsymbol{r} \cdot d\boldsymbol{r} = dx_1^2 + dx_2^2 + dx_3^2 \tag{A1b}$$

In an absolute time analysis, one takes dl to be the same in different reference frames; the frames can be accelerating relative to each other. One refers to dl as the spatial metric or the spatial length. In a relativistic time analysis, one takes $d\tau$ to be the same in different frames; again, the frames can be accelerating relative to each other. One refers to $cd\tau$ as the spacetime metric or the spacetime length. In Eq. (A1), c is the speed of light, τ is the proper time, t is the relativistic time, and l is the spatial length, in which x_1, x_2, and x_3 are rectangular coordinates. The position vector is $\boldsymbol{r} = x_1\boldsymbol{i}_1 + x_2\boldsymbol{i}_2 + x_3\boldsymbol{i}_3$, where $\boldsymbol{i}_1$, $\boldsymbol{i}_2$, and $\boldsymbol{i}_3$ are unit vectors. Equation (A1a) is the ordinary space-time metric. By dividing it by $d\tau^2$, we obtain the Lorentz factor $\gamma = dt/d\tau = 1/\sqrt{1 - (v/c)^2}$, where $v = dl/dt$ is speed. In absolute (Newtonian) time, one assume that $dl \ll cdt$ from which the ordinary spacetime metric reduces to $t = \tau$. The Lorentz factor dictates the transition between absolute time and relativistic time. In absolute time, the velocity vector is $\boldsymbol{v} = d\boldsymbol{r}/dt$, and the acceleration vector is $\boldsymbol{a} = d\boldsymbol{v}/dt$. In relativistic time, the relativistic velocity vector is $\boldsymbol{v}_R = d\boldsymbol{r}/d\tau$, and the relativistic acceleration vector is $\boldsymbol{a}_R = d\boldsymbol{v}_R/d\tau$. The velocity vector is $\boldsymbol{v} = v_1\boldsymbol{i}_1 + v_2\boldsymbol{i}_2 + v_3\boldsymbol{i}_3$, the relativistic velocity vector is $\boldsymbol{v}_R = v_{R1}\boldsymbol{i}_1 + v_{R2}\boldsymbol{i}_2 + v_{R3}\boldsymbol{i}_3$, the acceleration vector is $\boldsymbol{a} = a_1\boldsymbol{i}_1 + a_2\boldsymbol{i}_2 + a_3\boldsymbol{i}_3$, and the relativistic acceleration vector is $\boldsymbol{a}_R = a_{R1}\boldsymbol{i}_1 + a_{R2}\boldsymbol{i}_2 + a_{R3}\boldsymbol{i}_3$. With the Lorentz factor, it follows from Eq. (1) that the velocity vector and the relativistic velocity vector are related by

$$\boldsymbol{v}_R = \gamma\boldsymbol{v}, \quad \boldsymbol{v} = \frac{1}{\gamma}\boldsymbol{v}_R \tag{A2}$$

Let us now determine the relationships between the acceleration vector and the relativistic acceleration vector. First, we express the relativistic acceleration vector in terms of the velocity and acceleration vectors. The individual steps are

1) Invoke the product and chain rules:

$$\boldsymbol{a}_R = \frac{d\boldsymbol{v}_R}{d\tau} = \frac{dt}{d\tau}\frac{d}{dt}(\gamma\boldsymbol{v}) = \gamma\left(\frac{d\gamma}{t}\boldsymbol{v} + \gamma\boldsymbol{a}\right)$$

2) Starting with the definition of the Lorentz factor, recognize that the square of the magnitude of the velocity vector is $v^2 = \boldsymbol{v} \cdot \boldsymbol{v} = v_1^2 + v_2^2 + v_3^2$, and invoke the product and chain rules:

$$\frac{d\gamma}{dt} = \frac{d}{dt}\left(1 - \left(\frac{v}{c}\right)^2\right)^{-1/2} = \frac{d}{dt}\left(1 - \frac{\boldsymbol{v} \cdot \boldsymbol{v}}{c^2}\right)^{-1/2}$$

$$= -\frac{1}{2}\left(1 - \frac{\boldsymbol{v} \cdot \boldsymbol{v}}{c^2}\right)^{-3/2}\left(-\frac{\boldsymbol{v} \cdot \boldsymbol{a} + \boldsymbol{a} \cdot \boldsymbol{v}}{c^2}\right)$$

$$= -\frac{1}{2}\left(1 - \frac{\boldsymbol{v} \cdot \boldsymbol{v}}{c^2}\right)^{-(3/2)}\left(-2\frac{\boldsymbol{v} \cdot \boldsymbol{a}}{c^2}\right) = \gamma^3\frac{\boldsymbol{v} \cdot \boldsymbol{a}}{c^2}$$

3) Finally, substitute step 2 into step 1 and rearrange terms:

$$\boldsymbol{a}_R = \gamma\left(\frac{d\gamma}{dt}\boldsymbol{v} + \gamma\boldsymbol{a}\right) = \gamma\left(\gamma^3\boldsymbol{v}\frac{\boldsymbol{v} \cdot \boldsymbol{a}}{c^2} + \gamma\boldsymbol{a}\right)$$

$$= \gamma^2\left(\boldsymbol{a} + \frac{\gamma^2}{c^2}(\boldsymbol{v} \cdot \boldsymbol{a})\boldsymbol{v}\right)$$

Done.

Next, we derive the inverse relationship, that is, the acceleration vector in terms of the relativistic velocity and acceleration vectors.

4) Take the dot product of $\boldsymbol{v}$ and $\boldsymbol{a}_R$ in step 3, and form a common denominator:

$$\boldsymbol{v} \cdot \boldsymbol{a}_R = \boldsymbol{v} \cdot \gamma^2\left(\boldsymbol{a} + \frac{\gamma^2}{c^2}(\boldsymbol{v} \cdot \boldsymbol{a})\boldsymbol{v}\right) = \gamma^2(\boldsymbol{v} \cdot \boldsymbol{a})\left(1 + \gamma^2\left(\frac{v}{c}\right)^2\right)$$

$$= \gamma^2(\boldsymbol{v} \cdot \boldsymbol{a})\left(1 + \frac{1}{1 - \left(\frac{v}{c}\right)^2}\left(\frac{v}{c}\right)^2\right)$$

$$= \gamma^2\frac{\boldsymbol{v} \cdot \boldsymbol{a}}{1 - \left(\frac{v}{c}\right)^2}\left(1 - \left(\frac{v}{c}\right)^2 + \left(\frac{v}{c}\right)^2\right) = \gamma^4\boldsymbol{v} \cdot \boldsymbol{a}$$

5) Finally, substitute step 4 in to step 3 and solve for $\boldsymbol{a}$:

$$\boldsymbol{a}_R = \gamma^2\left(\boldsymbol{a} + \frac{\gamma^2}{c^2}(\boldsymbol{v} \cdot \boldsymbol{a})\boldsymbol{v}\right) = \gamma^2\left(\boldsymbol{a} + \frac{\gamma^2}{c^2}\frac{1}{\gamma^4}(\boldsymbol{v} \cdot \boldsymbol{a}_R)\boldsymbol{v}\right)$$

$$= \gamma^2\boldsymbol{a} + \frac{1}{c^2}(\boldsymbol{v} \cdot \boldsymbol{a}_R)\boldsymbol{v}$$

$$\boldsymbol{a} = \frac{1}{\gamma^2}\left(\boldsymbol{a}_R - \frac{1}{c^2}(\boldsymbol{v} \cdot \boldsymbol{a}_R)\boldsymbol{v}\right)$$

Done.
Steps 1 through 5 determined the relationships between the acceleration vector and the relativistic acceleration vector, which are again

$$\boldsymbol{a}_R = \gamma^2\left(\boldsymbol{a} + \frac{\gamma^2}{c^2}(\boldsymbol{a} \cdot \boldsymbol{v})\boldsymbol{v}\right) \tag{A3a}$$

$$\boldsymbol{a} = \frac{1}{\gamma^2}\left(\boldsymbol{a}_R - \frac{1}{c^2}(\boldsymbol{v} \cdot \boldsymbol{a}_R)\boldsymbol{v}\right) \tag{A3b}$$

b. Spherical Coordinates

We now express the spacetime metric, the velocity and acceleration components, and Eq. (A3b) in terms of spherical coordinates; the radial coordinate is r, the polar coordinate is θ, and the azimuthal coordinate is ϕ. In terms of spherical coordinates, the rectangular coordinates are

$$x_1 = rs_\theta c_\phi, \quad x_2 = rs_\theta s_\phi, \quad x_3 = rc_\theta \tag{A4}$$

In Eq. (A4), we used the abbreviated notation $s_\theta = \sin\theta$, $c_\theta = \cos\theta$, $s_\phi = \sin\phi$, and $c_\phi = \cos\phi$. First, we determine the spacetime metric in spherical coordinates.

1) By differentiation of Eq. (A4), the increments of the rectangular coordinates are

$$dx_1 = s_\theta c_\phi dr + rc_\theta c_\phi d\theta - rs_\theta s_\phi d\phi,$$

$$dx_2 = s_\theta s_\phi dr + rc_\theta s_\phi d\theta + rs_\theta c_\phi d\phi,$$

$$dx_3 = c_\theta dr - s_\theta d\theta$$

2) From step 1, expand, regroup, and cancel terms given that $1 = s_\theta^2 + c_\theta^2$, and that $1 = s_\phi^2 + c_\phi^2$ to express dl^2 in spherical coordinates:

$$dl^2 = dx_1^2 + dx_2^2 + dx_3^2 = (s_\theta c_\phi dr + rc_\theta c_\phi d\theta - rs_\theta s_\phi d\phi)^2$$

$$+ (s_\theta s_\phi dr + rc_\theta s_\phi d\theta + rs_\theta c_\phi d\phi)^2 + (c_\theta dr - s_\theta d\theta)^2$$

$$= (s_\theta^2 c_\phi^2 + s_\theta^2 s_\phi^2 + c_\theta^2)dr^2 + (c_\theta^2 c_\phi^2 + c_\theta^2 s_\phi^2 + s_\theta^2)r^2 d\theta^2$$

$$+ (s_\phi^2 + c_\phi^2)r^2 s_\theta^2 d\phi^2 + (2s_\theta c_\phi c_\theta c_\phi + 2s_\theta s_\phi c_\theta s_\phi$$

$$- 2c_\theta s_\theta)rdrd\theta + (-2s_\theta c_\phi s_\theta s_\phi + 2s_\theta s_\phi s_\theta c_\phi)rdrd\phi$$

$$+ (-2c_\theta c_\phi s_\theta s_\phi + 2c_\theta s_\phi s_\theta c_\phi)r^2 d\theta d\phi$$

$$= dr^2 + r^2 d\theta^2 + r^2 s_\theta^2 d\phi^2$$

3) Finally, substitute step 2 into Eq. (A1a) to get the spacetime metric in spherical coordinates:

$$c^2 d\tau^2 = c^2 dt^2 - dl^2 \qquad (A5a)$$

$$dl^2 = dr^2 + r^2 d\theta^2 + r^2 \sin^2\theta d\phi^2 \qquad (A5b)$$

Done.

Next, assume that the motion is planar by letting $x_3 = 0$ ($\theta = \pi/2$), and express the velocity and acceleration components in terms of r and ϕ.

1) From Eq. (A4), the radial and circumferential unit vectors are

$$\boldsymbol{n}_r = \frac{\boldsymbol{r}}{r} = \frac{1}{r}(x_1 \boldsymbol{i}_1 + x_2 \boldsymbol{i}_2) = c_\phi \boldsymbol{i}_1 + s_\phi \boldsymbol{i}_2, \boldsymbol{n}_\phi = -s_\phi \boldsymbol{i}_1 + c_\phi \boldsymbol{i}_2$$

2) By time differentiation in step 1

$$\frac{d\boldsymbol{n}_r}{dt} = (-s_\phi \boldsymbol{i}_1 + c_\phi \boldsymbol{i}_2)\frac{d\phi}{dt} = \frac{d\phi}{dt}\boldsymbol{n}_\phi,$$

$$\frac{d\boldsymbol{n}_\phi}{dt} = (-c_\phi \boldsymbol{i}_1 - s_\phi \boldsymbol{i}_2)\frac{d\phi}{dt} = -\frac{d\phi}{dt}\boldsymbol{n}_r$$

3) From step 2, the velocity vector and its r and ϕ components are

$$\boldsymbol{v} = v_r \boldsymbol{n}_r + v_\phi \boldsymbol{n}_\phi = \frac{d\boldsymbol{r}}{dt} = \frac{d}{dt}(r\boldsymbol{n}_r) = \frac{dr}{dt}\boldsymbol{n}_r + r\frac{d\phi}{dt}\boldsymbol{n}_\phi,$$

$$v_r = \frac{dr}{dt}, \quad v_\phi = r\frac{d\phi}{dt}$$

4) Finally, from step 2 and step 3, the acceleration vector is

$$\boldsymbol{a} = a_r \boldsymbol{n}_r + a_\phi \boldsymbol{n}_\phi = \frac{d\boldsymbol{v}}{dt} = \frac{d}{dt}(v_r \boldsymbol{n}_r + v_\phi \boldsymbol{n}_\phi)$$

$$= \left(\frac{dv_r}{dt} - v_\phi\frac{d\phi}{dt}\right)\boldsymbol{n}_r + \left(v_r\frac{d\phi}{dt} + \frac{dv_\phi}{dt}\right)\boldsymbol{n}_\phi$$

$$= \left(\frac{d^2r}{dt^2} - r\left(\frac{d\phi}{dt}\right)^2\right)\boldsymbol{n}_r + \left(\frac{dr}{dt}\frac{d\phi}{dt} + \frac{dr}{dt}\frac{d\phi}{dt} + r\frac{d^2\phi}{dt^2}\right)\boldsymbol{n}_\phi$$

$$= \left(\frac{d^2r}{dt^2} - r\left(\frac{d\phi}{dt}\right)^2\right)\boldsymbol{n}_r + \left(r\frac{d^2\phi}{dt^2} + 2\frac{dr}{dt}\frac{d\phi}{dt}\right)\boldsymbol{n}_\phi$$

Done.

Abbreviate a derivative with respect to time t by an over dot. The velocity vector, the acceleration vector, and their components given previously are

$$\boldsymbol{v} = \dot{r}\boldsymbol{n}_r + r\dot{\phi}\boldsymbol{n}_\phi, \quad v_r = \dot{r}, \quad v_\phi = r\dot{\phi} \qquad (A6)$$

$$\boldsymbol{a} = (\ddot{r} - r\dot{\phi}^2)\boldsymbol{n}_r + (r\ddot{\phi} + 2\dot{r}\dot{\phi})\boldsymbol{n}_\phi, a_r = \ddot{r} - r\dot{\phi}^2,$$
$$a_\phi = r\ddot{\phi} + 2\dot{r}\dot{\phi} \qquad (A7)$$

Next, develop the expressions for the r and ϕ components of the relativistic velocity vector and the relativistic acceleration vector. We maintain the same r and ϕ coordinates and the same corresponding unit vectors $\boldsymbol{n}_r$ and $\boldsymbol{n}_\phi$ for relativistic quantities as for nonrelativistic quantities because the position vector is the same in both descriptions; there is just one spatial geometry. It follows that the steps taken that led to Eqs. (A6) and (A7) for $\boldsymbol{v}$ and $\boldsymbol{a}$ are the same as the steps that will lead to $\boldsymbol{v}_R$ and $\boldsymbol{a}_R$ except that the differentiations will be with respect to proper time τ instead of time t. Abbreviate a derivative with respect to proper time τ by a prime. Instead of Eqs. (A6) and (A7), one now obtains

$$\boldsymbol{v}_R = r'\boldsymbol{n}_r + r\phi'\boldsymbol{n}_\phi, \quad v_{Rr} = r', \quad v_{R\phi} = r\phi' \qquad (A8)$$

$$\boldsymbol{a}_R = (r' - r\phi'^2)\boldsymbol{n}_r + (r\phi' + 2r'\phi')\boldsymbol{n}_\phi, \ a_{Rr} = r' - r\phi'^2,$$
$$a_{R\phi} = r\phi' + 2r'\phi' \qquad (A9)$$

Finally, express Eq. (A3b) in terms of r and ϕ.

1) The individual terms in Eq. (A3b), expressed in terms of r and ϕ, are

$$\boldsymbol{v} = v_r \boldsymbol{n}_r + v_\phi \boldsymbol{n}_\phi, \ \boldsymbol{a} = a_r \boldsymbol{n}_r + a_\phi \boldsymbol{n}_\phi, \ \boldsymbol{a}_R = a_{Rr}\boldsymbol{n}_r + a_{R\phi}\boldsymbol{n}_\phi$$

2) From step 1

$$\boldsymbol{v} \cdot \boldsymbol{a}_R = (v_r \boldsymbol{n}_r + v_\phi \boldsymbol{n}_\phi) \cdot (a_{Rr}\boldsymbol{n}_r + a_{R\phi}\boldsymbol{n}_\phi) = v_r a_{Rr} + v_\phi a_{R\phi}$$

3) Substitute the terms in step 1 and step 2 into Eq. (A3b):

$$a_r \boldsymbol{n}_r + a_\phi \boldsymbol{n}_\phi = \frac{1}{\gamma^2}\Bigg(a_{Rr}\boldsymbol{n}_r + a_{R\phi}\boldsymbol{n}_\phi$$
$$- \frac{1}{c^2}(v_r a_{Rr} + v_\phi a_{R\phi})(v_r \boldsymbol{n}_r + v_\phi \boldsymbol{n}_\phi)\Bigg)$$

4) The radial and circumferential components in step 3 are

$$a_r = \frac{1}{\gamma^2}\left(a_{Rr} - \frac{1}{c^2}(v_r a_{Rr} + v_\phi a_{R\phi})v_r\right)$$

$$a_\phi = \frac{1}{\gamma^2}\left(a_{R\phi} - \frac{1}{c^2}(v_r a_{Rr} + v_\phi a_{R\phi})v_\phi\right)$$

5) From Eq. (A9) and step 4, Eq. (A7) are rewritten in the matrix–vector form:

$$\begin{pmatrix} a_r \\ a_\phi \end{pmatrix} = \frac{1}{\gamma^2}\begin{bmatrix} 1 - \left(\frac{v_r}{c}\right)^2 & -\left(\frac{v_r}{c}\right)\left(\frac{v_\phi}{c}\right) \\ -\left(\frac{v_r}{c}\right)\left(\frac{v_\phi}{c}\right) & 1 - \left(\frac{v_\phi}{c}\right)^2 \end{bmatrix}\begin{pmatrix} a_{Rr} \\ a_{R\phi} \end{pmatrix},$$

$$\begin{pmatrix} a_{Rr} \\ a_{R\phi} \end{pmatrix} = \begin{pmatrix} r' - r\phi'^2 \\ r' + 2r'\phi' \end{pmatrix}, \ \begin{pmatrix} a_r \\ a_\phi \end{pmatrix} = \begin{pmatrix} \ddot{r} - r\dot{\phi}^2 \\ r\ddot{\phi} + 2\dot{r}\dot{\phi} \end{pmatrix} \qquad (A10)$$

Done.

c. Spacetime Impetus

Spacetime impetus assumes the ordinary (Minkowski) spacetime framework developed earlier. In that framework, the governing equations are

$$\boldsymbol{R} = m\boldsymbol{a}_R \qquad (A11a)$$

$$\boldsymbol{F} = -\left(1 + 3\left(\frac{v_{R\phi}}{c}\right)^2\right)\frac{GMm}{r^3}\boldsymbol{r} \qquad (A11b)$$

Equation (A11a) expresses the principle of impetus, in which $\boldsymbol{R}$ is a resultant interaction force vector acting on a source. Equation (A11b) expresses a relativistic gravitational force vector by a stationary source of mass M that acts on a moving source of mass m, and where G is a universal gravitational constant. The term $1 + 3(v_{R\phi}/c)^2$ is the relativistic correction to the gravitational force. For the two-body problem. $\boldsymbol{R} = \boldsymbol{F}$.

d. General Relativity

General relativity assumes a curved (Riemannian) spacetime framework. Note that, in GR, for an isotropic source, the usual formulation of GR employs Schwarzschild coordinates [25]. Besides the singularity at $r = 0$, it has another singularity at the Schwarzschild radius $r = r_s$ (although its original formulation only had the one singularity at $r = 0$). Eddington–Finkelstein coordinates are one alternative

[26]. They suggest that the singularity in the Schwarzschild coordinates at r_s is not "physical." Kruskal–Szekeres coordinates [27] are another alternative. When using them, a body falling into a black hole crosses the event horizon, unlike when using the Schwarzschild coordinates. Gullstrand–Painlevé coordinates are yet another alternative [28,29]. They also eliminate the singularity at r_s. The different alternatives produce black holes that differ, and the differences have not yet been observed. These questions would not appear to impact interstellar travel unless one was getting close to a black hole.

In any event, its spacetime framework and governing equations are

$$0 = \delta \int c \, d\tau_G \tag{A12a}$$

where

$$c^2 d\tau_G^2 = \sum_{a=0}^{3} \sum_{b=0}^{3} g_{ab} dx_{Gb}^2 \tag{A12b}$$

Equation (A12a) expresses the principle of least action for an action that is equal to the speed of light c. Equation (A12b) gives the Riemannian (quadratic) spacetime metric, in which g_{ab} are coefficients that need to be determined. In Eq. (A12b), $x_{G0} = ct_G$, where t_G is a temporal coordinate and x_{G1}, x_{G2}, and x_{G3} are spatial coordinates. The principle of general covariance leads to the geodesic equations

$$0 = \frac{dx_{Ga}^2}{ds^2} + \sum_{c=0}^{3} \sum_{d=0}^{3} \Gamma_{cd}^a \frac{dx_{Gc}}{ds} \frac{dx_{Gd}}{ds} \tag{A13a}$$

$$\Gamma_{cd}^a = -\frac{1}{2} \sum_{b=0}^{3} g^{ab} \left(\frac{\partial g_{cb}}{\partial x_{Gd}} + \frac{\partial g_{db}}{\partial x_{Gc}} + \frac{\partial g_{cd}}{\partial x_{Gb}} \right) \tag{A13b}$$

Equation (A13a) governs the geodesic motion, and the metric coefficients g_{ab} are determined for a particular problem from Eq. (A13b) with conditions that satisfy the principle of light.

The first exact solution to Eq. (A13) was found by Schwarzschild for the two-body problem. The solution, called the Schwarzschild metric, is

$$c^2 d\tau_G^2 = \left(1 - \frac{r_s}{r_G}\right) c^2 dt_G^2 - \left(1 - \frac{r_s}{r_G}\right)^{-1} dr_G^2 - r_G^2 d\theta_G^2 - r_G^2 \sin^2 \theta_G d\phi_G^2 \tag{A14}$$

where $r_s = (2GM/c^2)$ is called the Schwarzschild radius. By dividing Eq. (A14) by $d\tau_G^2$, we set the action to

$$L = c^2 = \left(1 - \frac{r_s}{r_G}\right) c^2 t_G'^2 - \left(1 - \frac{r_s}{r_G}\right)^{-1} r_G'^2 - r_G^2 \theta_G'^2 - r_G^2 \sin^2 \theta_G \phi_G'^2 \tag{A15}$$

The solution to Eq. (A12) is then obtained by solving the associated Lagrange equations (for $\theta_G = \pi/2$):

$$\left(\frac{\partial L}{\partial t_G'}\right)' - \frac{\partial L}{\partial t_G} = 0 \,, \quad \left(\frac{\partial L}{\partial r_G'}\right)' - \frac{\partial L}{\partial r_G} = 0 \,, \quad \left(\frac{\partial L}{\partial \phi_G'}\right)' - \frac{\partial L}{\partial \phi_G} = 0 \tag{A16}$$

1) The derivatives of L in Eq. (A15) (for $\theta_G = \pi/2$) are

$$\frac{\partial L}{\partial t_G'} = 2\left(1 - \frac{r_s}{r_G}\right) c^2 t_G', \quad \frac{\partial L}{\partial r_G'} = -2\left(1 - \frac{r_s}{r_G}\right)^{-1} r_G',$$

$$\frac{\partial L}{\partial \phi_G'} = -2r_G^2 \phi_G', \quad \frac{\partial L}{\partial t_G} = 0,$$

$$\frac{\partial L}{\partial r_G} = \frac{r_s}{r_G^2} c^2 t_G'^2 + \left(1 - \frac{r_s}{r_G}\right)^{-2} \frac{r_s}{r_G^2} r_G'^2 - 2r_G \phi_G'^2, \quad \frac{\partial L}{\partial \phi_G} = 0$$

2) Substitute the derivatives in step 1 into Eq. (A16):

$$\left(\left(1 - \frac{r_s}{r_G}\right) t_G'\right)' = 0,$$

$$\left(\left(1 - \frac{r_s}{r_G}\right)^{-1} r_G'\right)' + \frac{1}{2}\left(\frac{r_s}{r_G^2} c^2 t_G'^2 + \left(1 - \frac{r_s}{r_G}\right)^{-2} \frac{r_s}{r_G^2} r_G'^2 - 2r_G \phi_G'^2\right) = 0,$$

$$(r_G^2 \phi_G')' = 0 \tag{A17}$$

3) The spatial part of the governing equations can be isolated from the temporal part of the governing equations, first by defining $u = 1/r_G$ and then by expressing u as a function of ϕ. The spatial governing equation is from Eq. (A17). The steps, which are given elsewhere (see [22] p. 208), yield

$$\frac{d^2 u}{d\phi_G^2} + u - \frac{3GM}{c^2} u^2 = \frac{GM}{h^2} \tag{A18a}$$

for constant

$$h = r v_{R\phi} \tag{A18b}$$

In Eq. (A7), h is the specific angular momentum of the two-body system. The solution applies to bodies that have an appreciable amount of mass down to bodies that travel at the speed of light for which $1/h$ tends to zero [22].

e.   Structure of the Proof

The ordinary spacetime metric in Eq. (A5) and the Schwarzschild metric in Eq. (A14) are both functions of four coordinates. The coordinates in SI are r, θ, ϕ, and t, and the coordinates in GR are r_G, θ_G, ϕ_G, and t_G. The coordinates r, θ, and ϕ, and r_G, θ_G, and ϕ_G are spatial coordinates, and t and t_G are temporal coordinates. Regardless of the distinction between spatial and temporal coordinates, in both ordinary and curved spacetime, the path of a trajectory of a point is a function of four coordinates. The number is the same, and so, broadly, one might expect there to exist a one-to-one mapping between the four coordinates in SI and GR, a mapping that essentially "deforms" the ordinary spacetime coordinates to produce curved spacetime coordinates. Indeed, although there has been a "historical separation" between ordinary spacetime and curved spacetime, one would logically expect them to be connected. The proof given as follows will reveal that in fact the spatial coordinates map to themselves; we will find that $r_G = r, \theta_G = \theta$, and $\phi_G = \phi$, leaving us with the need to find the mapping between relativistic time t and GR coordinate time t_G. Note, because the spatial coordinates map to themselves, there is no bending of space within a frame of reference; the relativistic effects are across frames of reference and result from the invariance of the speed of light (or equivalently the invariance of proper time) across these frames. In other words, it will turn out that we will only need to "deform" time.

Throughout the proof, note that SI knowledge is found in the ordinary spacetime apparatus, which is given in Eqs. (A1–A10), and the SI proposition, which is given in Eq. (A11), and that the GR knowledge is found in Eqs. (A12–A18). The proof deduces GR behavior from SI behavior, in other words, proves that they are the same.

There are a variety of ways of organizing the proof. We have chosen to separate the temporal aspects from the spatial aspects because it is perhaps more insightful this way. We will first determine the temporal map, as though we have already proven that the spatial coordinates map to themselves, and after that, we will determine the spatial map, proving that the spatial coordinates do indeed map to themselves. To determine the temporal map, we will start with the ordinary spacetime metric in Eq. (A5) and find how it transforms to the Schwarzschild metric in Eq. (A14). To determine the spatial map, we will start with the governing equations in SI and manipulate them into a spatial governing equation that is identical to the spatial equation in GR, Eq. (A18), proving that the spatial coordinates in SI and GR are the same.

f.   Temporal Map

The determination of the temporal map is as follows.

1) Set the spacetime metric in Eq. (A5a) equal to the curved spacetime metric in Eq. (A14) ($d\tau_G^2 = d\tau^2$). Also, let $r_G = r$, $\theta_G = \theta$, and $\phi_G = \phi$ to facilitate the derivation, as explained earlier:

$$c^2 dt^2 - dr^2 - r^2 d\theta^2 - r^2 \sin^2 \theta d\phi^2$$
$$= \left(1 - \frac{r_s}{r}\right) c^2 dt_G^2 - \left(1 - \frac{r_s}{r}\right)^{-1} dr^2 - r^2 d\theta^2 - r^2 \sin^2 \theta d\phi^2$$

2) Cancel the terms $-r^2 d\theta^2 - r^2 \sin^2 \theta d\phi^2$ on both sides of the equation:

$$c^2 dt^2 - dr^2 = \left(1 - \frac{r_s}{r}\right) c^2 dt_G^2 - \left(1 - \frac{r_s}{r}\right)^{-1} dr^2$$

3) Divide by dt^2 and solve for $(dt_G/dt)^2$:

$$c^2 - \left(\frac{dr}{dt}\right)^2 = \left(1 - \frac{r_s}{r}\right) c^2 \left(\frac{dt_G}{dt}\right)^2 - \left(1 - \frac{r_s}{r}\right)^{-1} \left(\frac{dr}{dt}\right)^2$$

$$1 - \frac{1}{c^2}\left(\frac{dr}{dt}\right)^2 + \frac{1}{c^2}\left(1 - \frac{r_s}{r}\right)^{-1}\left(\frac{dr}{dt}\right)^2 = \left(1 - \frac{r_s}{r}\right)\left(\frac{dt_G}{dt}\right)^2$$

$$\left(\frac{dt_G}{dt}\right)^2 = \frac{1}{1 - \frac{r_s}{r}}\left[1 - \frac{1}{c^2}\left(\frac{dr}{dt}\right)^2 + \frac{1}{c^2}\left(1 - \frac{r_s}{r}\right)^{-1}\left(\frac{dr}{dt}\right)^2\right]$$

$$= \frac{1}{1 - \frac{r_s}{r}}\left[1 + \frac{1}{c^2}\left(-1 + \frac{1}{1 - \frac{r_s}{r}}\right)\left(\frac{dr}{dt}\right)^2\right]$$

4) Form a common denominator and take the square root:

$$\left(\frac{dt_G}{dt}\right)^2 = \frac{1}{1 - \frac{r_s}{r}}\left[1 + \frac{1}{c^2}\frac{\frac{r_s}{r}}{1 - \frac{r_s}{r}}\left(\frac{dr}{dt}\right)^2\right],$$
$$\frac{dt_G}{dt} = \left\{\frac{1}{1 - \frac{r_s}{r}}\left[1 + \frac{1}{c^2}\left(\frac{\frac{r_s}{r}}{1 - \frac{r_s}{r}}\right)\left(\frac{dr}{dt}\right)^2\right]\right\}^{1/2}$$

Done.

g.   Spatial Map

The spatial map is determined as follows.

1) From Eq. (A11b), the r and ϕ components of the relativistic gravitational force vector in SI are

$$F_r = -G\frac{Mm}{r^2}\left(1 + 3\left(\frac{v_{R\phi}}{c}\right)^2\right), \quad F_\phi = 0$$

2) From Eq. (A11a), the r and ϕ components of the relativistic gravitational acceleration vector in SI are

$$a_{Rr} = -G\frac{M}{r^2}\left(1 + 3\left(\frac{v_{R\phi}}{c}\right)^2\right), \quad a_{R\phi} = 0$$

3) From step 2 and Eq. (A9)

$$r'' - r\phi'^2 = -G\frac{M}{r^2}\left(1 + 3\left(\frac{v_{R\phi}}{c}\right)^2\right)$$
$$0 = r\phi'' + 2r'\phi' \qquad\qquad \text{(A19)}$$

4) Invoke Eq. (A8) and define the specific angular momentum as $h = rv_{R\phi} = r^2\phi'$. Differentiate h with respect to proper time, invoke the product and chain rules, and from the second equation in step 3

$$h' = (r^2\phi')' = r^2\phi'' + 2rr'\phi' = r(r\phi'' + 2r'\phi') = 0 \quad \text{(A20)}$$

Thus, h is constant.

5) Let $u = 1/r$. Differentiate with respect to ϕ, invoke the power and chain rules, and step 4

$$\frac{du}{d\phi} = \frac{d}{d\phi}\left(\frac{1}{r}\right) = \frac{d}{d\phi}r^{-1} = -r^{-2}\frac{dr}{d\phi} = -r^{-2}\frac{dr}{d\tau}\frac{d\tau}{d\phi} = -\frac{1}{h}\frac{dr}{d\tau}$$

6) Differentiate again with respect to ϕ:

$$\frac{d^2u}{d\phi^2} = \frac{d}{d\phi}\left(-\frac{1}{h}\frac{dr}{d\tau}\right) = \frac{d\tau}{d\phi}\frac{d}{d\tau}\left(-\frac{1}{h}\frac{dr}{d\tau}\right) = -\frac{1}{h}\frac{d\tau}{d\phi}\frac{d^2r}{d\tau^2}$$
$$= -\frac{1}{r^2}\left(\frac{d\tau}{d\phi}\right)^2\frac{d^2r}{d\tau^2}$$

7) From step 5 and step 6

$$\frac{d^2u}{d\phi^2} + u = -\frac{1}{r^2}\left(\frac{d\tau}{d\phi}\right)^2\frac{d^2r}{d\tau^2} + \frac{1}{r} = -\frac{1}{r^2}\left(\frac{d\tau}{d\phi}\right)^2\left(\frac{d^2r}{d\tau^2} - r\left(\frac{d\phi}{d\tau}\right)^2\right)$$
$$= -\frac{1}{r^2}\left(\frac{d\tau}{d\phi}\right)^2 a_{Rr}$$

8) From step 7 and step 2

$$\frac{d^2u}{d\phi^2} + u = \frac{1}{r^2}\left(\frac{d\tau}{d\phi}\right)^2\frac{GM}{r^2}\left(1 + 3\left(\frac{v_{R\phi}}{c}\right)^2\right)$$
$$= \frac{1}{r^4}\left(\frac{d\tau}{d\phi}\right)^2 GM\left(1 + 3\left(\frac{v_{R\phi}}{c}\right)^2\right) = \frac{GM}{h^2}\left(1 + 3\left(\frac{h}{rc}\right)^2\right)$$
$$= \frac{GM}{h^2} + \frac{3GM}{c^2}u^2$$
$$\frac{d^2u}{d\phi^2} + u - \frac{3\,GM}{c^2}u^2 = \frac{GM}{h^2}$$

This is identically Eq. (A18). Thus, $r_G = r$, $\theta_G = \theta$, and $\phi_G = \phi$. End of proof

Appendix B: Spacetime Impetus: Numerical Verification

The prediction of the anomalous precession of Mercury is a fine example of a problem in which the speed of light has an effect on an orbiting body, albeit it is a very small effect. This problem was one of the first used to verify GR, and it was the first one used by SI during its development to verify that its results agree with those obtained in GR [17,21]. NASA's ongoing Parker Solar Probe is another body in a nominally elliptical orbit around the sun that precesses. It, too, serves as a fine tutorial problem for those who would like to implement SI and numerically verify the agreement between SI and GR. This appendix gives the details needed to set up and solve this problem by both SI and GR.

B.1.   SI Orbital Equations

From line 5 of Table 1, the acceleration components are

$$a_x = -\left(1 - \left(\frac{v}{c}\right)^2\right)\left(x\left(1 - \left(\frac{v_x}{c}\right)^2\right) - y\frac{v_x v_y}{c^2}\right)$$
$$\times \frac{GM}{r^3}\left(1 + 3\left(\frac{v_{R\phi}}{c}\right)^2\right)$$
$$a_y = -\left(1 - \left(\frac{v}{c}\right)^2\right)\left(-x\frac{v_x v_y}{c^2} + y\left(1 - \left(\frac{v_y}{c}\right)^2\right)\right)$$
$$\times \frac{GM}{r^3}\left(1 + 3\left(\frac{v_{R\phi}}{c}\right)^2\right) \tag{B1}$$

where

$$r = \sqrt{x^2 + y^2}, \quad v_{R\phi} = \frac{\gamma}{r}(-yv_x + xv_y), \quad v = \sqrt{v_x^2 + v_y^2},$$
$$\gamma = \frac{1}{\sqrt{1 - \left(\frac{v}{c}\right)^2}}$$

It is understood that $x = x(t), y = y(t), v_x = v_x(t), v_y = v_y(t)$, $a_x = a_x(t)$, and $a_y(t)$. For purposes of numerical integration, for which position and velocity components are calculated forward in time, we rewrite the acceleration components in state-variable form as four first-order differential equations in terms of the state variables:

$$z_1(t) = x, \quad z_2(t) = y, \quad z_3(t) = v_x, \quad z_4(t) = v_y \tag{B2}$$

Substituting Eq. (B2) into Eq. (B1), the SI state equations are

$$\frac{dz_1}{dt} = z_3$$
$$\frac{dz_2}{dt} = z_4$$
$$\frac{dz_3}{dt} = -\left(1 - \left(\frac{v}{c}\right)^2\right)\left(z_1\left(1 - \left(\frac{z_3}{c}\right)^2\right) - z_2\frac{z_3 z_4}{c^2}\right)$$
$$\times \frac{GM}{r^3}\left(1 + 3\left(\frac{v_{R\phi}}{c}\right)^2\right)$$
$$\frac{dz_4}{dt} = -\left(1 - \left(\frac{v}{c}\right)^2\right)\left(-z_1\frac{z_3 z_4}{c^2} + z_2\left(1 - \left(\frac{z_4}{c}\right)^2\right)\right)$$
$$\times \frac{GM}{r^3}\left(1 + 3\left(\frac{v_{R\phi}}{c}\right)^2\right) \tag{B3}$$

where

$$r = \sqrt{z_1^2 + z_2^2}, \quad v_{R\phi} = \frac{\gamma}{r}(-z_2 z_3 + z_1 z_4),$$
$$v = \sqrt{z_3^2 + z_4^2}, \quad \gamma = \frac{1}{\sqrt{1 - \left(\frac{v}{c}\right)^2}}$$

B.2.   GR Orbital Equations

The classic differential equation in GR that describes the spatial behavior of a massive particle [22] is again (Eq. (A18))

$$\frac{d^2u}{d\phi^2} = \frac{3GM}{c^2}u^2 - u + \frac{GM}{h^2} \tag{B4}$$

where $u(\phi) = 1/r(\phi)$ with the spherical coordinates r and ϕ in the equatorial plane. The specific relativistic angular momentum h, which is constant during the motion, is

$$h = r^2\frac{d\phi}{d\tau} = rv_{R\phi}$$

Note when $(r_s/r) \to 0$ that $(d\tau/dt) = \left(\sqrt{1 - \frac{r_s}{r}}\right)/\gamma$; in the Parker probe orbit we can let $(r_s/r) = 0$. Also, the following expression will be useful when setting up the initial conditions:

$$\frac{du}{d\phi} = -\frac{1}{r^2}\frac{dr}{d\phi} \tag{B5}$$

For purposes of numerical integration, for which the variables u and $du/d\phi$ are calculated forward in time, we rewrite Eq. (B4) in state-variable form in terms of the new state variables:

$$z_1(t) = u, \quad z_2(t) = \frac{du}{d\phi} \tag{B6}$$

Substituting Eq. (B6) into Eq. (B5), the GR state equations are

$$\frac{dz_1}{d\phi} = z_2$$
$$\frac{dz_2}{d\phi} = \frac{3GM}{c^2}z_1^2 - z_1 + \frac{GM}{h^2} \tag{B7}$$

Numerically, the GR state equations are just about as simple to solve as the SI state equations. However, both conceptually and mathematically, this can be misleading. For one, Eq. (B7) follows from a complicated mathematical apparatus that is unique to GR, in which one deduces geodesic equations from a Schwarzschild metric [see the steps from Eqs. (A12–A17)] after which Eq. (B4) is derived [22]. Of course, Eq. (B4) only provides spatial information; it is missing temporal information (time, velocities, and accelerations). To find them, one goes back to the geodesic equations. Also, in SI, we find that one can transform from one frame to another by the Lorentz transformation. Finally, the SI methodology must be regarded as a relativistic extension of NT, drawing directly from the different principles already employed in nonrelativistic mechanics (principles of linear and angular momentum, work and energy, least action, the concept of force, etc.), which makes it more familiar.

B.3.   Numerical Data

Table B1 shows the orbital data for Mercury and the Parker probe. These data can be used to predict the orbit and, more specifically, the precession of the orbits of Mercury and the Parker probe. Here, we will focus on the Parker probe. The SI and GR simulations of the Parker probe are started at the perihelion position where the probe is closest to the sun and moving the fastest. Its initial conditions, in terms of the state variables, are

For SI:

$$z_1(0) = x(0) = 6.859788 \times 10^9 \text{ m}, \quad z_2(0) = y(0) = 0,$$
$$z_3(0) = v_x(0) = 0, \quad z_4(0) = v_y(0) = 190.8 \times 10^3 \text{ m/s}$$

Table B1   Mercury and Parker probe data

	Mercury	Parker probe
Mass m, kg	3.3022×10^{23}	50
Perihelion radius r_p, m	4.60012×10^{10}	6.859788×10^9
Semimajor axis A, m	57.91×10^9	57.766×10^9
Eccentricity e of the orbit	0.20566	0.881
Perihelion velocity v_p, m/s	58.98×10^3	190.800×10^3
Orbital period T	87.969 Earth days = 7,600,530 s	88 Earth days = 7,603,200 s

For GR:

$$z_1(0) = u(0) = \frac{1}{6.859788 \times 10^9} \, \text{m}^{-1}, \quad z_2(0) = \frac{du}{d\phi}(0) = 0$$

$$h(0) = r(0)v_{R\phi}(0)$$

$$= 6.859788 \times 10^9 \times \frac{190.8 \times 10^3}{\sqrt{1 - (190.8 \times 10^3 / 2.99 \times 10^8)^2}} \, \frac{\text{m}^2}{\text{s}}$$

B.4.   Results

Figure B1 shows the SI simulation of slightly more than one orbit of the Parker probe. The precession of the orbit is present but not visible on the scale of this plot. The derivative of the orbital radius r is calculated with respect to time t in the vicinity of the second perihelion. Figure B2 is the "precession plot," where the azimuthal angle $\delta\varphi$ is plotted just past 2π. We know the orbit is at the second perihelion when $(dr/dt) = 0$. For the Parker probe, this occurred at $\delta\varphi = 2.17 \times 10^{-6}$ rad. Note that Mercury has a precession angle per orbit of $\delta\varphi = 5.047 \times 10^{-7}$ rad, which is an order of magnitude smaller.

It is perhaps best to use a very accurate and reliable numerical ODE solver for the SI and GR problems. In MATLAB, the ODE 45 solver is recommended, while in Maple the DVERK78 solver is very good.

Note that these precession values are due only to relativistic effects. We ignore the tugs of other planets, solar oblateness, solar radiation, orbit maneuvers, etc. Of course, when reverting back to nonrelativistic mechanics, there is no precession at all ($\delta\varphi = 0$ rad).

Because of the equivalence of SI and GR, one can check the numerical value obtained previously by SI for the precession of the Parker probe from the GR formula $\delta\phi = 6\pi G(M + m)/c^2 A(1 - e^2)$ to get 2.17×10^{-6} rad/orbit.

The MAPLE codes that simulate the trajectories employing both the SI and GR equations of motion are available on GitHub [30].

References

[1] Patterson, M. J., and Benson, S. W., "NEXT Ion Propulsion System Development Status and Capabilities," NASA/TM—2008-214988, 2008; also AIAA Paper 2007-5199, July 2007.

[2] Mason, L., and Gibson, M., "Kilowatt-Class Fission Power Systems for Science and Human Precursor Missions," NASA/ TM 2013-216541, NETS–2013–6814, 2013.

[3] Zubrin, R. M., and Andrews, D. G., "Magnetic Sails and Interplanetary Travel," *Journal of Spacecraft and Rockets*, Vol. 28, No. 2, March–April 1991, pp. 197–203.
https://doi.org/10.2514/3.26230

[4] Manchester, Z., and Loeb, A., "Stability of a Light Sail Riding on a Laser Beam," *Astrophysical Journal Letters*, Vol. 837, No. 2, 2017, p. L20.
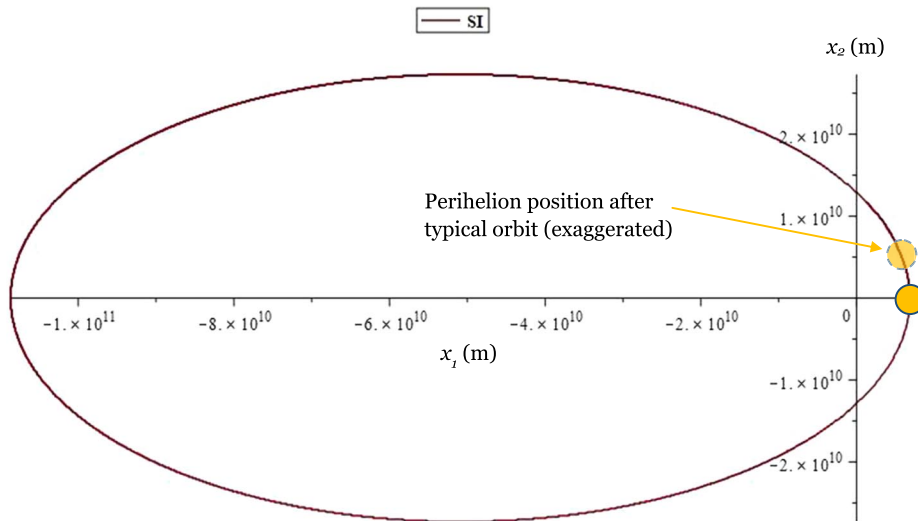https://doi.org/10.3847/2041-8213/AA619B

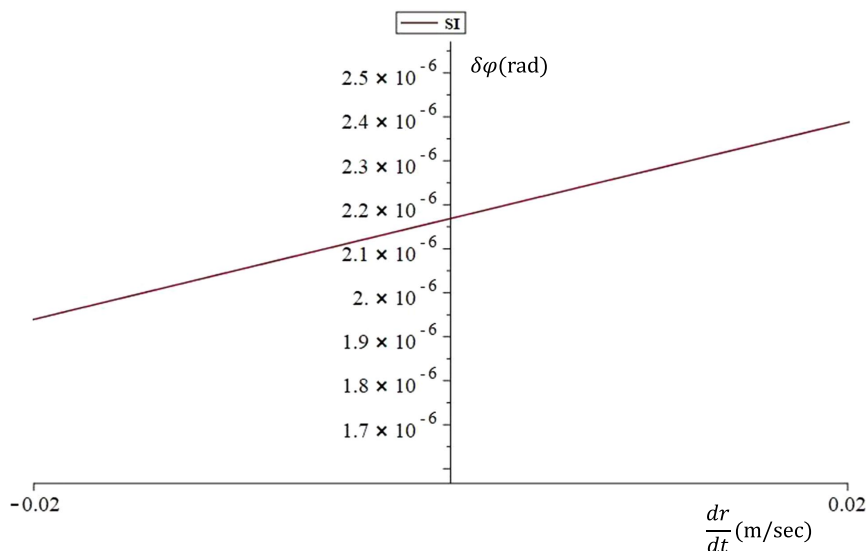**Fig. B1   Final orbit of the Parker probe.**

Fig. B2   Parker probe precession.

[5] Hoang, T., Lazarian, A., Burkhart, B., and Loeb, A., "The Interaction of Relativistic Spacecrafts with the Interstellar Medium," *Astrophysical Journal*, Vol. 837, No. 1, 2017, p. 5
https://doi.org/10.3847/1538-4357/aa5da6

[6] Santi, G., Favaro, G., Corso, A. J., Lubin, P., Bazzan, M., Ragazzoni, R., Garoli, D., and Pelizzo, M. G., "Multilayers for Directed Energy Accelerated Lightsails," *Communications Materials*, Vol. 3, No. 1, 2022, p. 16.
https://doi.org/10.1038/s43246-022-00240-8

[7] Ledingham, K. W. D., McKenna, P., and Singhal, R. P., "Applications for Nuclear Phenomena Generated by Ultra-Intense Lasers," *Science*, Vol. 300, No. 5622, May 2003, pp. 1107–1111.
https://doi.org/10.1126/science.1080552

[8] Parkin, K. L. G., "The Breakthrough Starshot System Model," *Acta Astonautica*, Vol. 152, Nov. 2018, pp. 370–384.
https://doi.org/10.1016/j.actaastro.2018.08.035

[9] Jackson, A., "Dispersion Analysis of Small-Scale-Spacecraft Interstellar Trajectories," *TVIW Conference*, Lunar and Planetary Inst., Houston, TX, 2017, pp. 1–14.
https://doi.org/10.13140/RG.2.2.18043.41762

[10] Fuzfu, A., Dhelonga-Biarufu, W., and Welcomme, O., "Sailing Toward the Stars Close to the Speed of Light," *Physical Review Research*, Vol. 2, No. 4, 2020, Paper 043186.
https://doi.org/10.1103/PhysRevResearch.2.043186

[11] Savage, B. D., and Mathis, J. S., "Observed Properties of Interstellar Dust," *Annual Review of Astronomy and Astrophysics*, Vol. 17, No. 1, 1979, pp. 73–111.
https://doi.org/10.1146/annurev.aa.17.090179.000445

[12] Draine, B. T., "Interstellar Dust Grains," *Annual Review of Astronomy & Astrophysics*, Vol. 41, No. 1, 2003, pp. 241–289.
https://doi.org/10.1146/annurev.astro.41.011802.094840

[13] Landgraf, W. J., Baggaley, W. J., Grün, E., Krüger, H., and Linkert, G., "Aspects of the Mass Distribution of Interstellar Dust Grains in the Solar System from In Situ Measurements," *Journal of Geophysical Research: Space Physics*, Vol. 105, No. A5, May 2000, pp. 10,343–10,352.
https://doi.org/10.1029/1999JA900359

[14] Min, M., Waters, L. B. F. M., de Koter, A., Hovenier, J. W., Keller, L. P., and Markwick-Kemper, F., "The Shape and Composition of Interstellar Silicate Grains," *Astronomy & Astrophysics*, Vol. 462, No. 2, 2007, pp. 667–676.
https://doi.org/10.1051/0004-6361:20065436

[15] Anon., "Parker Solar Probe," Feb. 2021, https://www.nasa.gov/content/goddard/parker-solar-probe [retrieved 4 Aug. 2023].

[16] Sebastián, A., Acedo, L., and Moraño, J. A., "An Orbital Model for the Parker Solar Probe Mission: Classical vs Relativistic Effects," *Advances in Space Research*, Vol. 70, No. 3, 2022, pp. 842–853.
https://doi.org/10.1016/j.asr.2022.05.037

[17] Silverberg, L. M., and Eischen, J. W., "Theory of Spacetime Impetus," *Physics Essays*, Vol. 34, No. 4, 2021, pp. 548–563.
https://doi.org/10.4006/0836-1398-34.4.548

[18] Pauli, W., *Theory of Relativity*, Vol. 165, Fundamental Theories of Physics, Dover New York, 1981, p. 272 (in German, 1921).

[19] Einstein, A., Infeld, L., and Hoffmann, B., "The Gravitational Equations and the Problem of Motion," *Annals of Mathematics*, Vol. 39, No. 1, 1938, pp. 65–100.
https://doi.org/10.2307/1968714.JSTOR 1968714

[20] Ziefle, R. G., "On the New Theory of Gravitation (NTG)," *Physics Essays*, Vol. 24, No. 2, 2011, pp. 213–239.
https://doi.org/10.4006/1.3567412

[21] Silverberg, L. M., and Eischen, J. W., "On a New Field Theory Formulation and a Space-Time Adjustment that Predict the Same Precession of Mercury and the Same Bending of Light as General Relativity," *Physics Essays*, Vol. 33, No. 4, 2020, pp. 489–512.
https://doi.org/10.4006/0836-1398-33.4.489

[22] Hobson, M. P., Efstathiou, G., and Lasenby, A. N., *General Relativity*, Cambridge Univ. Press, Cambridge, England, U.K., 2006, pp. 572.
https://doi.org/10.1063/1.2718760

[23] Cartan, E. O., "On Manifold with Affine Connection and the Theory of General Relativity (First Part)," *Scientific Annals of the Ecole Normale Supérieure*, Vol. 40, 1923, pp. 325–412.
https://doi.org/10.24033/asens.751

[24] Havas, P., "Four-Dimensional Formulations of Newtonian Mechanics and Their Relation to the Special and the General Theory of Relativity," *Reviews of Modern Physics*, Vol. 36, No. 4, Oct. 1964, p. 938.
https://doi.org/10.1103/RevModPhys.36.938

[25] Schwarzschild, K., "Über das Gravitationsfeld eines Massenpunktes nach der Einsteinschen Theorie," *Sitzungsberichte der Königlich Preussischen Akademie der Wissenschaften*, Vol. 7, 1916, pp. 189–196; also "On the Gravitational Field of a Mass Point According to Einstein's Theory" (in English Schwarzschild, Karl. "65. On the Gravitational Field of a Point Mass according to the Einsteinian Theory". A Source Book in Astronomy and Astrophysics, 1900–1975, edited by Kenneth R. Lang and Owen Gingerich, Cambridge, MA and London, England: Harvard University Press, 1979, pp. 451–455. https://doi.org/10.4159/harvard.9780674366688.c71).
https://doi.org/10.48550/arXiv.physics/9905030.

[26] Penrose, R., "Gravitational Collapse and Space-Time Singularities," *Physical Review Letters*, Vol. 14, No. 3, 1965, pp. 57–59.
https://doi.org/10.1103/PhysRevLett.14.57

[27] Kruskal, M. D., "Maximal Extension of Schwarzschild Metric," *Physical Review*, Vol. 119, No. 5, 1960, Paper 1743.
https://doi.org/10.1103/PhysRev.119.1743

[28] Gullstrand, A., "Allgemeine Lösung des statischen Einkörperproblems in der Einsteinschen Gravitationstheorie," *Arkiv för Matematik, Astronomi och Fysik*, Vol. 16, No. 8, 1922, pp. 1–15; also "General Solution of the Static One-Body Problem in Einstein's Theory of Gravitation" (in English).

[29] Painlevé, P., "La mécanique classique et la théorie de la relativité," *Comptes Rendus Academie des Sciences*, Vol. 173, 1921, pp. 677–680; also "Classical Mechanics and the Theory of Relativity" (in English).

[30] Eischen, J. W., "Spacetime Maple Codes," 2023, https://github.com/jweischen/Spacetime-Impetus-Maple-Codes [retrieved 4 Aug. 2023].

C. N. McGrath
Associate Editor